Aus dem Institut für Biosynthese Neuraler Strukturen
des Zentrums für Molekulare Neurobiologie Hamburg
des Universitätsklinikums Hamburg- Eppendorf
Direktorin Frau Prof. M. Schachner

EXPRESSION AND DISTRIBUTION OF KIR3.2 INTERACTION PARTNERS

Dissertation

Zur Erlangung des Grades eines Doktors der Medizin
dem Fachbereich Medizin der Universität Hamburg vorgelegt von

Mirja Mossekel
aus Hamburg

Hamburg, 2005

Aus dem Institut für Biosynthese Neuraler Strukturen
des Zentrums für Molekulare Neurobiologie Hamburg
des Universitätsklinikums Hamburg- Eppendorf
Direktorin Frau Prof. M. Schachner

EXPRESSION AND DISTRIBUTION OF KIR3.2 INTERACTION PARTNERS

Dissertation

Zur Erlangung des Grades eines Doktors der Medizin
dem Fachbereich Medizin der Universität Hamburg vorgelegt von

Mirja Mossekel
aus Hamburg

Hamburg, 2005

Angenommen vom Fachbereich Medizin der Universität Hamburg am 19.07.2003.

Veröffentlicht mit Genehmigung des Fachbereichs Medizin der Universität Hamburg.

Prüfungsausschuss: Der/ die Vorsitzende
Prüfungsausschuss: 2. Gutachter/ in
Prüfungsausschuss: 3. Gutachter/ in

TABLE OF CONTENTS

I. OBJECTIVE OF THE STUDY

The objective of this study is to characterize putative Kir3.2 interaction partners with regard to their expression and distribution in the mouse model.

Previous studies in our group have shown that the neuronal cell adhesion molecule NCAM regulates the surface delivery of Kir3.2 potassium channels (Delling et al., 2002). However, the underlying mechanism of this surface delivery has not yet been identified. The present results suggest that neither a direct interaction of NCAM and Kir3.2 nor the activation of commonly known NCAM signaling pathways are controlling the surface expression of Kir3.2. Furthermore, the mechanisms by which Kir3 channels are delivered to and inserted into the plasma membrane are poorly understood. One of the hypotheses for the NCAM-mediated regulation is the existence of an interaction partner for Kir3.2 involved in the regulation of surface expression.

Two potential Kir3.2 binding partners were found when using the Kir3.2 C-terminus as bait in a Yeast Two-Hybrid screening system: MUPP1 and FILIP. Only little is known about the expression patterns and tissue distribution of these molecules with respect to RNA and protein levels.

We therefore performed Western Blot analysis, *In Situ* hybridization, and Immunohistochemistry analysis for Kir3.2, MUPP 1, and FILIP, and compared regions of putative co-expression, since co-expression in the same cell is the minimal requirement for putative Kir3.2/MUPP and Kir3.2/FILIP interaction.

II. INTRODUCTION

The Central Nervous System (CNS) of mammals consists of more than 10^{12} neurons, forming a multitude of synaptic contacts.
Understanding the underlying molecular mechanisms of the forming of specific synapses and their remodeling throughout life, i.e. synaptic plasticity, remains one of neurobiology's greatest challenges.
Cell recognition and intercellular communication are essential for synaptic finding and bonding. During synaptogenesis and as a part of the learning and regenerational process, axons and dendrites connect with other neurons, with glia cells, cells of sensoric organs, muscles, and with the extracellular matrix.
It is a group called "cell adhesion molecules" which is responsible for the forming of correct connections between neurons. Furthermore, these cell adhesion molecules have a strong impact on neurite outgrowth, cell migration, and cell survival.
They can be classified into four groups:

- Integrins (Hynes, 1992; Reichardt and Tomaselli, 1991)
- Calcium-depending Cadherins (Kemler and Ozawa, 1989; Takeichi, 1991)
- Extracellular Matrix Molecules (Reichardt and Tomaselli, 1991; Sanes, 1989)
- Immunoglobin (Ig) superfamily of cell surface glycoproteins (Bruemmendorf and Rathjen, 1993; Williams and Barclay, 1988)

1.0 The Neural Cell Adhesion Molecule NCAM

NCAM belongs to the immunoglobin superfamily of cell recognition molecules which is characterized by the presence of several Ig-modules in the extracellular domain. The prototypical examples of this family are antibodies (Edelman et al., 1969) and MHC-antigens (Orr et al., 1979). Many of these Ig-molecules in the immune system, such as the T-cell receptor (Kronenberg et al., 1986), are involved in highly specific cell-cell recognition events (Springer, 1990). Many, if not most cell-recognition molecules in the nervous system, such as NCAM and L1, are composed not only of Ig-modules, but combine them with other repeated structures. One of these structures is the fibronectin repeat of the subtype III (FNIII-domain).

NCAM was the first Ig-like cell adhesion molecule to be isolated and characterized in detail (Brackenbury et al., 1977; Cunningham et al., 1987; Hoffman et al., 1982; Thiery et al., 1977). It forms the prototype of neural adhesion molecules of the Ig-superfamily.

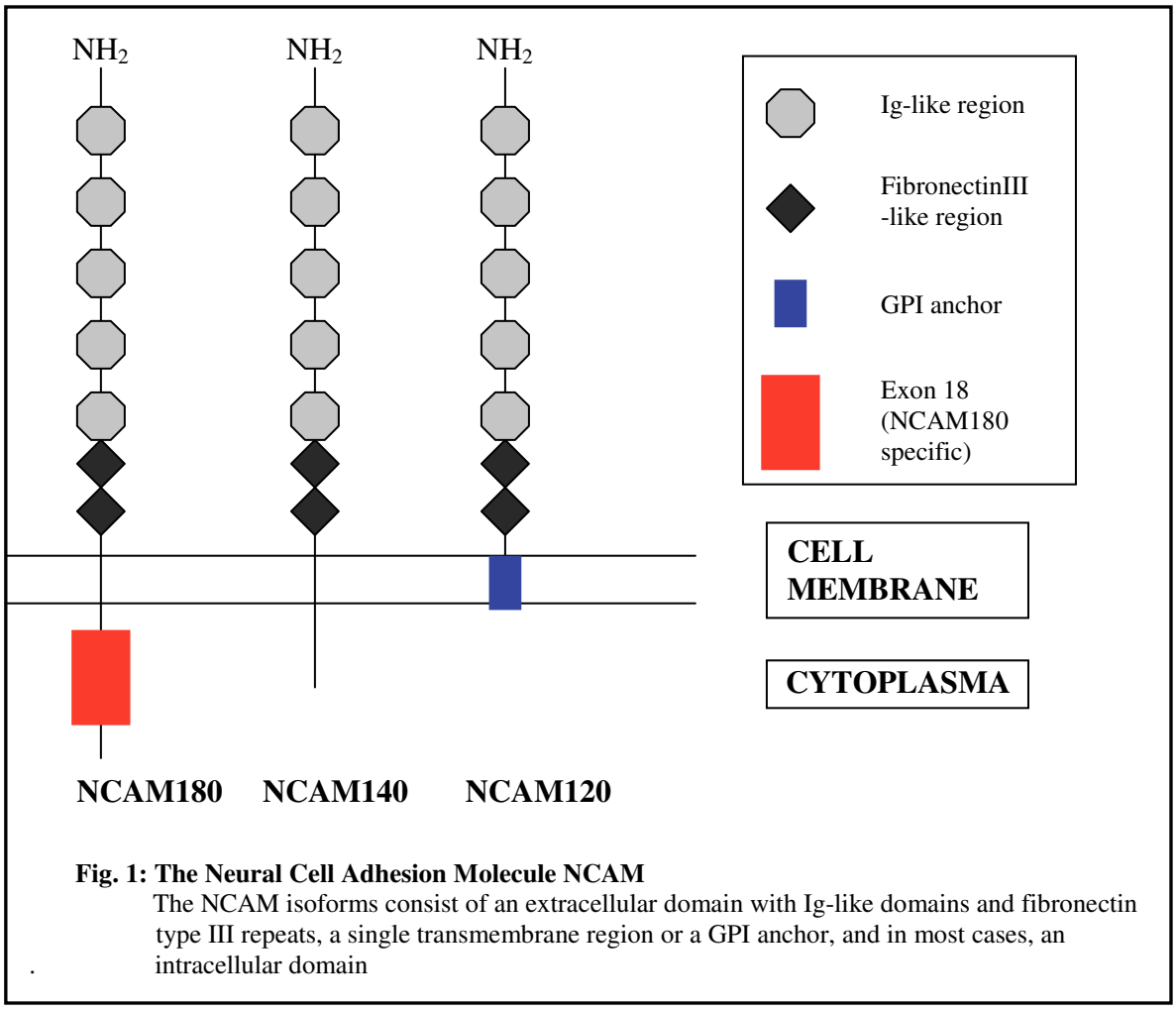

Fig. 1: The Neural Cell Adhesion Molecule NCAM
The NCAM isoforms consist of an extracellular domain with Ig-like domains and fibronectin type III repeats, a single transmembrane region or a GPI anchor, and in most cases, an intracellular domain

Several NCAM proteins are encoded by a single gene. Diversity of NCAM proteins is generated at different levels, including transcriptional and posttranslational modifications. Three major isoforms are generated by alternative splicing of a primary transcript leading to the translation of three proteins that have apparent molecular masses of 120, 140, and 180 kD, designated NCAM120, NCAM140, and NCAM180, respectively (Cunningham et al, 1987). (see Fig. 1).

Homologues with the same domain composition, biochemical and functional properties have been identified in rodents, chickens, and humans. Potential species homologues are fasciclin II in *Drosophila* and apCAM in *Aplysia* (reviewed by Bruemmendorf and Rathjen, 1994). The expression of alternatively spliced forms of NCAM, in terms of time and cell-type specificity, is regulated differentially (for review, see Jorgensen, 1995).

Several posttranslational modifications of NCAM proteins are known, such as phosphorylation of serine and threonine residues (Mackie et al., 1989). The physiological relevance of these intracellular modifications has so far not been elucidated.

1.1 NCAM-mediated Signal Transduction

The extracellular domain of NCAM mediates various Ca^{2+} independent cell-cell and cell-extracellular matrix interactions, involved in proliferation, cell migration, neurite outgrowth, axon fasciculation, and synaptic remodeling (Cremer et al., 1997; Doherty et al., 1990; Doherty et al., 1992; Doherty and Walsh, 1992; Fields and Itoh, 1996; Jorgensen, 1995; Rutishauser and Jessell, 1988; Schachner, 1991; Sporns et al., 1995).
NCAM shows homophilic binding with a high rate of cooperativity, so that a 2-fold increase in NCAM level can increase adhesiveness more than 30-fold (Hoffman and Edelman, 1983). In an heterophilic interaction, NCAM can bind heparin, a major component of the extracellular matrix (Cole et al., 1986a; Cole et al., 1986b; Cole and Glaser, 1986), and soluble NCAM, derived from proteolytic cleavage near the membrane, can bind to collagen I-VI and IX (Probstmeier et al., 1989). Furthermore, NCAM assists homophilic binding of another cell recognition molecule (L1) in “cis” configuration, that is, on the same cell membrane (Kadmon et al., 1990a; Kadmon et al., 1990b).
It has been shown that the unglycosylated core protein and even single domains can perform many of the cell recognition functions of NCAM. Of the three major NCAM isoforms, all have been found to serve as neuritogenic ligands (Doherty et al., 1989; Doherty et al., 1990) due to their identical amino acid sequence of extracellular domains.
First attempts to elucidate the molecular events underlying NCAM mediated neuritogenesis have attributed a fundamental role to the fibroblast growth factor (FGF) receptor (Williams et al., 1995). Over-expression of a truncated FGF receptor-1 with a deleted kinase domain inhibited neurite outgrowth of PC12 cells when cultured on NCAM presenting fibroblasts (Saffell et al., 1997). The ability of NCAM to promote neurite outgrowth was therefore suggested to depend solely on the interaction between the extracellular domains of NCAM and the FGF receptor.
The view that the FGF receptor is the only mediator of NCAM-dependent signal transduction had to be abolished when new data showed that NCAM-dependent neurite outgrowth is also impaired in cultured neurons from mice deficient in the non-receptor

tyrosine kinase fyn (Beggs et al., 1994). Moreover, immunoprecipitation studies revealed an association of a minor portion of NCAM140 but not NCAM180 with fyn (Beggs et al., 1997). Although the two signaling mechanisms would appear distinct at first sight, there is evidence that both the FGF-receptor pathway and the fyn-FAK pathway are operant in PC12-cells (Kolkova et al., 2000a).

Furthermore, NCAM stimulation has been shown to activate the transcription factor NFκ B in cultured astrocytes and cerebellar neurons (Krushel et al., 1999). Both NCAM-mediated neurite outgrowth and NFκ B activation could be partially blocked by the overexpression of a NCAM cytoplasmatic domain construct (Kolkova et al., 2000b; Little et al., 2001). This finding indicated that the overexpressed domain exerted a dominant negative effect on NCAM-induced signal transduction and suggested that an intracellular interaction of this domain is involved in the signaling process.

1.2 NCAM-mediated Surface Localization of Kir3.2

A putative modulation of potassium channels by NCAM and its homologues could involve a cytoplasmatic interaction as well: Thomas et al. (1997) identified FasII, the *Drosophila* homologue of NCAM, to cluster shaker K^+ channels in the cell membrane via the intracellular PDZ (see Chapter 3) protein discs-large (dlg).

The shaker K^+ channel, which belongs to the group of voltage-gated potassium channels, and FasII bind via their intracellular domains to dlg, which mediates a co-localization of the two molecules. While the co-clustering with FasII obviously does not change single channel properties of the K^+ channel, the interaction is thought to be relevant for the structural organization of the synapse. However, this co-localization has not been observed for the mammalian homologues of fasII and dlg, namely NCAM and SAP-97 (Thomas et al., 1997).

Delling et al. (2002) have shown, that in hippocampal neurons of NCAM $^{-/-}$ mice, Kir3 currents were increased by ~240% compared to wild type neurons, or in other words, in the presence of NCAM, Kir3 currents were reduced by ~40% compared to hippocampal neurons in which NCAM was absent. Since neither internalization nor protein expression of Kir3 channels were affected by NCAM140, it was suggested that NCAM140 regulates the transport of the Kir3 channels to the membrane.

In search of the signaling mechanisms by which NCAM controls the Kir3 channel delivery, neither acute stimulation of NCAM nor kinase inhibitors, that are known to mediate NCAM signaling, affected Kir3 inhibition rates. Furthermore, NCAM140 and the Kir3 channels did not physically associate with each other in the cell membrane. However, it was shown for the first time that both NCAM140 and Kir3.1/3.2 channels are localized in detergent-resistant microdomains, also called lipid rafts. The existence of a common binding partner, similar to dlg, shared by Kir3.2 and NCAM, was suggested.

Using the Kir3.2 C-terminus as bait in the Yeast-Two-Hybrid-System, our lab isolated the Filamin A interacting protein FILIP (see Chapter 6) as a binding partner for Kir3.2 and PDZ protein MUPP1 (see Chapter 4) as a binding partner for both NCAM and Kir3.2 (Delling, M., personal message, 2003). Co-immunoprecipitation and pull-down assays from transiently transfected CHO cells verify these findings. These results may present the missing link to understanding the way in which NCAM regulates cell surface localization of Kir3.2.

As a physiological consequence of this regulatory mechanism, it is conceivable that a reduced Kir3 channel activity during periods of NCAM protein up-regulation, such as development and increase of synaptic strength induced by learning and memory, increases the impedance of postsynaptic membranes and thus induces neurons to become more sensitive to synaptic activation (Delling et al., 2002).

2.0 Inwardly Rectifying Potassium Channels (Kir Channels)

The molecular nature of inwardly rectifying potassium (Kir) channels was discovered in 1993, when the first two subunits (ROMK1/Kir1.1 and IRK1/Kir2.1) were cloned (Ho et al., 1993; Kubo et al., 1993). Since then, a large number of Kir proteins have been identified and grouped into a potassium channel gene family (see Tab. 1).

K^+ channels formed out of Kir subunits elicit currents, which flow more readily in the inward than in the outward direction (Fakler et al., 1995), thus hyperpolarizing the membrane potential, cause inhibitory effects (Luescher et al., 1997).

These K^+ channels play pivotal roles in the maintenance of the resting membrane potential, in the regulation of the action potential, in receptor-dependent inhibition of cellular excitability and in secretion and absorption of K^+ ions across cell membrane.

SUBFAMILIES	SUBTYPES	CHANDY AND GUTMAN NOMENCLATURE
Classical inwardly rectifying K^+ channels	IRK1, IRK2, IRK3	Kir2.1, Kir2.2, Kir2.3
G-protein activated K^+ channels	GIRK1, GIRK2, GIRK3, GIRK4	Kir3.1, Kir3.2, Kir3.3. Kir3.4
ATP sensitive K^+ channels	uK_{ATP}-1, BIR	Kir6.1, Kir6.2
ATP depending K^+ channels	ROMK1 K_{AB}-2	Kir1.1a Kir4.1
Others	BIR9	Kir5.1, Kir7.1

Table 1: Summary of the different Kir subunits identified to date

The best known examples of the physiological importance of Kir regulation are the ATP dependence of Kir6 channels in the control of insulin secretion (Ashcroft et al., 1984; Ashcroft and Rorsman, 1989) and the determination of myocardial resistance to hypoxia (Friedrich et al., 1990), the regulation of Kir3 channels by G-proteins to account for the vagal control of heart rate (Krapivinsky et al., 1995; Wickman and Clapham, 1995), and the regulation of Kir1 channels by intracellular K^+ and pH, which controls K^+ secretion in the kidney (Wang et al., 1997).

Protein kinase A and protein kinase C as well as tyrosine kinases, such as src kinase, regulate a variety of ion channels. For the Kir channels, the effects of such kinases on the K^+ current amplitude have been observed by many authors (Cohen et al., 1996; DiMagno et al., 1996; Fakler et al., 1994; Henry et al., 1996; McNicholas et al., 1994; Wischmeyer and Karschin, 1996). Some of these effects, such as current stimulation by activation of PKA, are common to all members of the Kir family and are not correlated to a particular phosphorylation site in the primary sequences. This may be due to the influence of kinases on other regulatory pathways, such as the phosphatidylinositol pathway. Other effects are highly specific to the respective subunit, such as the effect of PKC on Kir2.3 (Henry et al., 1996) and the nerve growth factor receptor-mediated tyrosine phosphorylation of the Kir2.1 subunit (Wischmeyer et al., 1998).

But phosphorylation does not only seem to alter current amplitude in ion channels, but seems to also have an effect on ion channel trafficking within the cell. Ma et al. (2002) have reported specific trafficking signals embedded within ion channels, that is, amino acid sequence motifs that are crucial to channel membrane targeting and assembly. These trafficking signals also seem to be regulated by phosphorylation. The results suggest that the surface expression of Kir3.2 channels can e.g. be dynamically regulated by the phosphorylation state of the channel: at the Kir3.2 C- terminal Ser-Thr phosphorylation site, a mutation of Thr to Ala leads to reduced Kir3.2 surface localization. Mutation of Thr to Asp, however, mimics the phosphorylated state of the channel, leading to enhanced Kir3.2 surface localization (Ma et al., 2002).

2.1 G-Protein-activated Inwardly Rectifying Potassium Channels (Kir3)

In contrast to the constitutively active Kir1 and Kir2 groups, more than one subunit seems to be required in Kir3 channels to form a normal functional channel; Kir3 channels are thus heterotetramers (see Fig. 2). Kir3.1 alone does not produce functional channels when expressed in most cell lines tested (Chan et al., 1996b) and is not delivered to the cell membrane when transfected alone into oocytes (Stevens et al., 1997). Kir3.2 and Kir3.4 alone form G-protein-gated channels in various heterologous expression systems, but with rather aberrant single channel properties. The presence of Kir3.1 corrects the single channel properties to yield open times and amplitudes similar to those observed in cardiac and nerve cells (Lesage et al., 1995).

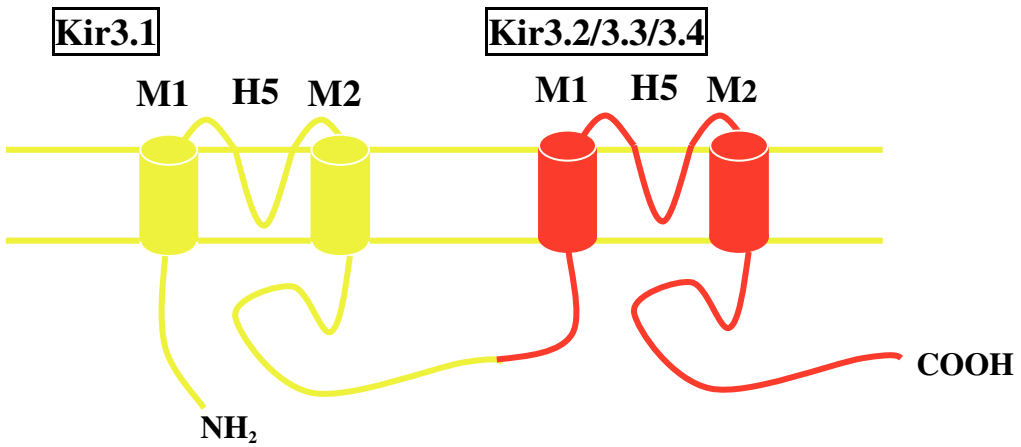

Fig. 2: Schematic drawing of a Kir3 channel. All Kir subunits consist of two transmembrane regions M1 and M2 and a pore forming region (H5). Both the NH_2- and the COOH-terminus are located intracellularly.

The Kir3.1 subunit co-purifies with Kir3.2 and Kir3.4 (Chan et al., 1996a; Lesage et al., 1995) and has been shown to form functional channels with all other Kir3 subunits in heterologous expression systems (Mark and Herlitze, 2000; Isomoto et al., 1997). However, other studies also report functional Kir3.2 homomers and Kir3.2/3.3 combinations (Inanobe et al., 1999; Jelacic et al., 2000; Wischmeyer et al., 1997). Kir3.1, Kir3.2 and Kir3.3 subunits are abundantly expressed in several brain areas (Karschin and Karschin, 1997) and Kir3.1/3.2 and Kir3.1/3.3 channels are believed to be the main functional Kir3 combinations in the brain (Luescher et al., 1997; Kofuji et al., 1995). In contrast, Kir3.4 subunits are mainly expressed in the heart (Karschin and Karschin, 1997) and form the atrial K(Ach) channels together with the Kir3.1 subunit. The Kir3.1/3.2 and Kir3.1/3.3 channels are thus commonly referred to as the neuronal Kir3 channels, whereas the Kir3.1/3.4 channel is depicted as the cardiac Kir3 channel.

The main stimulatory effect on Kir3 channels is caused by the $G_{\beta\gamma}$ subunit of the heterotrimeric G-protein that binds to Kir3 channels and activates them (Huang et al., 1995; Slesinger et al., 1995; Wickman and Clapham, 1995). Inhibition of Kir3 channels by G_{α} has also been described (Slesinger et al., 1995).

3.0 PDZ Domain containing Proteins

In the past years, PDZ domains have emerged as important protein-protein interaction modules that bind in a sequence-specific fashion to short C-terminal peptides or internal peptides that fold in a β-finger.

PDZ domains were originally recognized as ~90 amino acid-long repeated sequences in the synaptic protein ***P***SD-95 (postsynaptic density-95), in the *Drosophila* septate junction protein ***D***lg (discs-large), and in the epithelial tight junction protein ***Z***O-1 (zonula occludens-1), hence the acronym PDZ (Sheng and Sala, 2001).

PDZ-domain containing proteins can be classified into three families (see fig. 3). The first family consists of proteins made up entirely of PDZ domains, e.g. Syntenin and NHERF (N^+/ H^+ exchanger regulating factor). PSD-95, Discs-large, and ZO-1 belong to the second family of proteins also called membrane-associated guanylate kinases (MAGUKs), which contain a SH3 domain and a guanylate kinase-like (GK) domain in their C-terminal region in addition to up to three PDZ domains in the N-terminal half. The third family includes proteins that contain not only several PDZ domains, but also other protein domains, such

as L27-, WW-, C2-, or PH-domains. MUPP1 is an example of this family, consisting of 13 PDZ domains plus a N-terminal L27-domain (Nourry, 2003).

PDZ-containing proteins are found in a variety of organisms, both procaryotic and eucaryotic. They are abundantly represented in *Caenorhabditis elegans* (60 PDZ-containing proteins are encoded in its genome), *Drosophila melanogaster* (69 encoded PDZ-containing proteins), and mammalian genomes. In humans, as many as 400 PDZ-domain containing proteins have been identified so far.

PDZ domains all have a similar architecture, consisting of six antiparallel β-strands (βA-βF) and two α-helices (αA and αB), their overall fold approximates a six-strand β-sandwich flanked by two α-helices.The N-and C-termini of the PDZ domain lie close to each other on the opposite side of the domain relative to the peptide-binding groove, an arrangement common to protein interaction modules (Sheng and Sala, 2001).

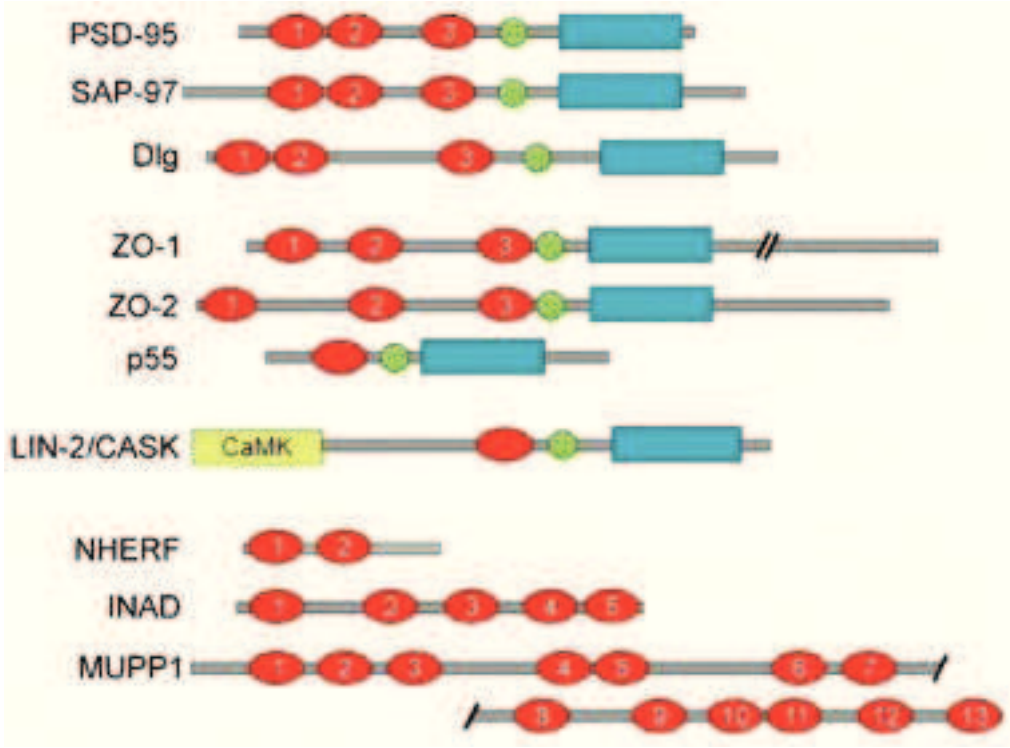

Fig. 3: Examples of PDZ domain containing proteins. The picture shows the domain structure of several PDZ proteins. PDZ domains are depicted as ovals, SH3 domains as circles, guanylate kinase domains as rectangles (taken from "PDZ domains and the organization of supramolecular complexes", Sheng and Sala, 2001).

The architecture of the PDZ domains is designed for binding to a free C-terminal peptide. The carboxylate-binding loop in the binding-groove extends from a highly conserved arginine or lysine residue to the signature Gly-Leu-Gly-Phe (GLGF), a motif typical of PDZ domains.

The three main-chain amide protons of the GLGF motif can now form hydrogen bonds with the terminal carboxylate of the peptide. It is thus the GLGF motif which specifically recognizes the C-terminal peptides. The carboxylate-binding loop (R/K-XXX-GLGF) between βA and βB is highly conserved among PDZ domains. The second and fourth residues of the GLGF motif are invariably hydrophobic. The third residue is absolutely conserved, whereas a serine, threonine, or proline can replace the first glycine in a minority of PDZ domains (Sheng and Sala, 2001). The residues lining the binding groove are united in their hydrophobic character, leading to the generalization that most (if not all) PDZ domains choose to bind peptides with a hydrophobic C-terminal residue.

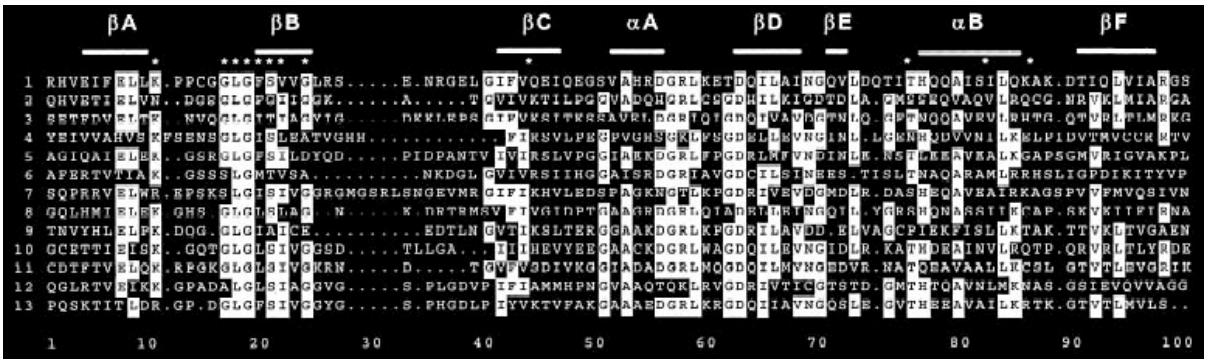

Fig. 4: Sequence analysis of MUPP1 as an example of PDZ containing proteins.
Conserved amino acids are shown in black (>50%), the secondary structure is written at the top (taken from "Cloning and characterization of MUPP1, a novel PDZ domain protein", Ullmer et al., 1998).

The C-terminal residues of PDZ binding motifs are highly conserved on positions –2 and 0. Especially position –2, interacting with the first αB residue (αB1), appears to be of great significance and can thus be used to group peptides into three classes of PDZ binding motifs (see tab. 2).

Consensus sequences for PDZ binding are often written as a C-terminal tripeptide. Based on structural studies, however, it is clear that PDZ domains interact specifically with at least a C-terminal tetrapeptide. It is therefore more accurate to describe PDZ binding

consensus sequences in terms of four amino acids, such as E/Q-T/S-X-V for PSD-95 (Doyle et al., 1996).

Nuclear magnetic resonance studies suggest that as many as six residues of the Fas C-terminus interact with PDZ-containing protein PTP1E (Kozlov et al., 2000). Songyang et al. (1997) even found that residues up to position –8 are required for specific binding.

It is also known, that internal peptides that fold in a β-hairpin structure can also bind to PDZ domains. The Ca^{2+} channel TRP (transient receptor potential) uses this mechanism to bind one PDZ domain of INAD (inactivation-no-after potential D) (Chevesich et al., 1997). Many PDZ domains can bind a surprising number of ligands in a sequence specific way, although these may not contain the same C-terminal residue (Sheng and Sala, 2001). INAD can e.g. bind three different ligands with both domain 3 and domain 4 (Shawn Xu et al., 1998). And the number of putative ligands can still be considerably higher.

Class	C-terminal sequence	interacting protein	PDZ-domain-protein
Class I			
X-S or T-X-V	E-T-D-V	Shaker potassium channel	PSD-95
	D-S-W-V	δ–Catenin	Erbin
X-S or T-X-L	D-S-S-L	β2-adrenergic receptor	NHERF (PDZ1)
	D-T-R-L	CFTR	NHERF (PDZ1)
Class II			
X-Ψ–X-Ψ	E-Y-Y-V	Neurexin	CASK
	E-Y-F-I	Glycophorin C	p55
Class III			
X-D oder E-X-Ψ	V-D-S-V	Melatonin receptor	nNOS
	G-E-P-L	KIF17	mLIN10

Table 2: Classification of PDZ domains according to their specificity for C-terminal peptides (taken from "PDZ domain proteins: plug and play!", Nourry et al., 2003).

The interaction between PDZ domain and ligand may be influenced in several ways. The –2 residue of PDZ-binding C-terminal peptides, the most critical site for PDZ recognition as mentioned above, is frequently a phosphorylable amino acid such as threonine or serine. The –2 residue of Kir2.3 can e.g. be phosphorylated by protein kinase A

(PKA). This phosphorylation abolishes Kir2.3 interaction with PSD-95 (Cohen et al., 1996).

Furthermore, the interaction of a ligand with its cell surface receptor may then again influence its interaction with the PDZ domain containing protein. E.g. NHERF only binds β_2-adrenergic receptors when they are activated (Hall et el., 1998).

It has been shown for a number of PDZ domain containing proteins that they can multimerize, i.e. connect e.g. the third and fourth domains of separate INAD proteins with each other (Shawn et al., 1998). Multimerization without participation of PDZ domains has also been described. PSD-95 appears to use its N-terminal region to bind other protein domains (Hsuehet al., 1997).

PDZ-containing proteins are typically involved in the assembly of supramolecular complexes that perform localized signaling functions at particular subcellular locations.

Organization around a PDZ-based scaffold allows the stable localization of interacting proteins and enhances the rate and fidelity of signal transduction within the complex (Kumar and Shieh, 2001; Shawn Xu et al., 1998).

PDZ domains that contain proteins can easily be strung together to form multiple PDZ proteins (e.g. INAD, GRIP) or can be combined with other modular protein interaction domains to generate more complex scaffolds (CASK/ LIN-2, PSD-95). Individual PDZ domains have different binding specificities, so that the combination of multiple PDZ domains increases both size and heterogeneity of the PDZ-based complex.

Since they recognize just a few amino acids at the C-termini of proteins, PDZ domains are able to interact with the great majority of transmembrane proteins that have their

C-termini facing the cytoplasma, such as cell surface receptors, channel proteins, and adhesion proteins, suggest a predominant role of PDZ proteins in signal transduction pathways.

3.1 PDZ-mediated Protein Trafficking

Some PDZ-containing proteins may not only be involved in arranging binding partners, but also in the trafficking of interacting proteins within the cell. PSD-95 e.g. clusters glutamate receptors and K^+ channels in the postsynaptic density of excitatory synapses (Sheng et al., 2001). This clustering at the cell surface may be related to inhibition of receptor internalization (Kim and Sheng, 2004), since removing the PSD95 binding motif

from the receptor protein NR2B leads to enhanced membrane internalization (Roche et al., 2001).

The same was shown for the Kv1.4 potassium channel and its PSD95 binding motif (Jugloff et al., 2000). Furthermore, PSD95 not only regulates the activity of interacting proteins by influencing membrane internalization, but even changes their intrinsic functional properties. PSD95 suppresses e.g. Kir2.3 activity by reducing its single channel conductance (Nehring et al., 2001).

Using the Kir3.2 C-terminal PDZ recognition sequence ESKV, it was shown in co-transfection assays that Kir3.2 has the capability of binding PSD95 *in vitro* (Inobe et al., 1999). Further experiments at the postsynaptic density of dendrites of dopaminergic substantia nigra neurons however did not reveal an *in vivo* Kir3.2/PSD95 interaction.

Inobe et al. (1999) thus suggested that the Kir3.2 recognition site may be used for binding to a different PDZ protein yet to be identified.

These data suggest, that our view of PDZ proteins has to evolve from one of static adaptors for clustering interaction partners to a more dynamic picture in which PDZ scaffolds organize ensembles of proteins, which change at different localizations within the cell and in response to neuronal activity, thus playing a substantial role in controlling the structure and plasticity of synapses (Kim and Sheng, 2004).

4.0 Multiple PDZ-containing Protein MUPP1

MUPP1 is a member of a family of PDZ domain-containing proteins, which includes INADL (INAD-like protein), CIPP (channel-interacting PDZ domain protein), and the putative *Caenorhabditis elegans* polypeptide C52A11.4.

MUPP1 consists of 13 PDZ domains, C52A11.4 of ten, INADL of seven, and CIPP of four PDZ domains (Bécamel et al., 2001). Neither of these proteins has a catalytic domain.

The PDZ domains of these four proteins reveal high sequence homology; MUPP1 and INADL show the strongest homology. Furthermore, similar PDZ domains are arranged in the same order from N- to C-terminus in all four proteins (see Fig. 5), implying a need for precise arrangement in order to assemble a functional macromolecular complex (Ullmer et al., 1998).

The segments between the PDZ domains are variable. MUPP1 may e.g. contain putative binding motifs for the SH3 domains of the adaptor-protein CRK1 (between PDZ domains 6 and 7) and Grb2 (between PDZ domains 7 and 8) (personal message from Schneeberger, D., 2003).

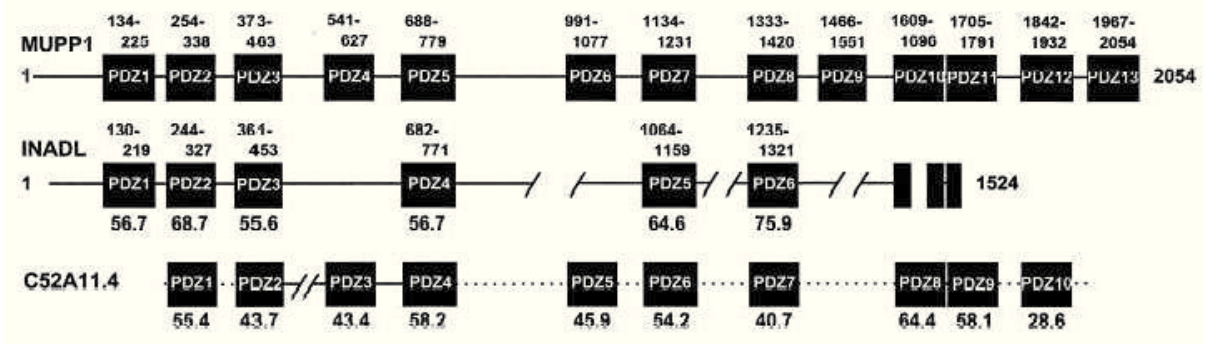

Fig. 5: Structure of MUPP1 and family members (taken from "Cloning and characterization of MUPP1, a novel PDZ domain protein", Ullmer et al., 1998).

4.1 MUPP1 Interaction Partners

MUPP1 was first described by Ullmer et al. in 1998. The C-terminus of 5-HT-$_{2C}$-receptor was used as bait in a Yeast-Two-Hybrid-System and MUPP1 could be identified as interaction partner (Ullmer et al., 1998). Later further members of the serotonine 5-HT-subfamily, that is 5-HT-$_{2A}$-receptor and 5-HT-$_{2B}$-receptor, were found to specifically also bind the 10th domain of MUPP1 (Bécamel et al., 2001). MUPP1 clusters 5-HT-$_{2C}$-receptors on the cell surface (Bécamel et al., 2001).

Ligand binding leads to phosphorylation of serine residues near the C-terminus of 5-HT-$_{2C}$-receptor. This abolishes MUPP1 interaction (Parker et al., 2003), implying that the modulation of binding capacities of MUPP1 binding motifs is a necessary step to regulate intracellular signal cascades.

Several other interaction partners of MUPP1 have been identified so far, including the human protooncogene c-Kit (Mancini et al., 2000), which interacts with PDZ domain 10.

Interaction between MUPP1 and c-Kit stops c-Kit activation, that is, autophosphorylation of cytoplasmatic domains (Mancini et al., 2000), so that successive steps in signal transduction are abolished. The physiological relevance of this interaction is still unknown.

A large group of MUPP1 binding partners are tight junction proteins such as the transmembrane protein subfamily of claudins. Hamazaki et al. (2001) showed that claudin-1 binds domain 10 of MUPP1 (Hamazaki et al., 2001). Later, claudin-8 was identified as a ligand for domain 9 (Jeansonne et al., 2003). Poliak et al. (2002) found MUPP1 to interact with claudin-5. Here, however, the interacting MUPP1 PDZ domain has not yet been characterized. The junctional adhesion protein JAM, a transmembrane protein of the Ig superfamily, specifically interacts with PDZ domain 9 (Hamazaki et al., 2001).

Lee et al. (2000) discovered that several oncoproteins derived from DNA tumor viruses bind MUPP1. E4-ORF1-oncoprotein from human adenovirus 9 binds domain 7 and 10, inducing an accumulation of MUPP1 in puncuate bodies in the cytoplasma, whereas MUPP1 would normally only accumulate at cell-cell-contacts (Lee et al., 2000). E4-ORF1-oncoprotein from human adenoviruses 5 and 12 can also bind MUPP1, possibly leading to the same accumulation (Lee et al., 2000). High-risk-papilloma virus (HPV18) oncoprotein E6 (18E6) also interacts with MUPP1. The exact PDZ domain has not yet been described. In contrast to E4-ORF1-oncoprotein, 18E6 induces MUPP1 degradation. MUPP1's half-life is decreased four-fold when linked to 18E6 (Lee et al., 2000). E6 oncoproteins from HPV31, -39,- 45, and –51 show identical PDZ binding motifs and are thus thought to be capable of binding MUPP1 with the same effect.

The findings of Lee et al. propose an involvement of MUPP1 in negatively regulating cellular proliferation.

With its 10^{th} and 13^{th} domain, MUPP1 also binds TAPP1 and TAPP2, two proteins which interact with the phosphatidylinositol-3.4-bisphosphate (PtdIns-3,4-P_2) pathway (Kimber et al., 2002). With the dopamine D_3-receptor (D_3R), Griffon et al. (2003) add yet another G-protein-coupled receptor to the list of putative interaction partners. Here, MUPP1 again acts as scaffolding protein, compartmentalizing D_3R with its interaction partner CLIC6 (chloride intracellular channel 6), which also binds MUPP1 (Griffon et al., 2003).

Using the Yeast-Two-Hybrid-System, our lab has isolated a further interaction partner for MUPP1, which is the potassium channel Kir3.2 (Delling, M. personal message, 2002) (see Chapter 2). It is PDZ domain 13, which specifically binds the ESKV motif at the Kir3.2 C-terminus. In further studies it was possible to show an interaction between MUPP1 and NCAM (Delling, M., personal message, 2003).

Since localizing cell surface molecules such as NCAM and ion channels such as Kir3.2 to specific subcellular sites can be crucial to proper functioning, these findings may present the missing link to understanding the way in which NCAM regulates cell surface localization of Kir3.2.

5.0 Filamins are Actin-binding Proteins

The cytoskeleton is indispensable for the control of cell shape, the mechanic stability of the cell, and the cell's resistance towards osmotic forces. It makes cell motility, cell division, organelle transport, and phagocytosis possible via dynamic reorganization.

Three different kinds of fibrillic elements make up the cytoskeleton: microtubuli, neurofilaments, and microfilaments. Microfilaments are the smallest of these macromolecules, they have a diameter of 3-5nm and consist of polymerized actin monomers.

The actin network is not a static object. A large number of actin-binding proteins can attach it to the cell membrane and can thus induce a change in actin architecture in response to signaling cascades. This may lead to an addition, loss, or polymerization of actin fibres.

Filamins form one group of actin binding proteins. They were first identified in 1975 in rabbit alveolar macrophages (Hartwig and Stossel, 1975). Since then, more filamins have been described, both in vertebrates and in invertebrates such as *Dictyostelium discoideum* or *Entamoeba histiolytica* (Condeelis et al., 1981; Condeelis et al., 1982; Vargas et al.,1996). In humans, three filamin genes have been identified: filamin A, B, and C (hsFLNA, hsFLNB, hsFLNC, respectively). The three encoded filamin proteins show an overall sequence homology of about 60-80% (Stossel et al., 2001). Filamin A and B are the most ubiquitously expressed filamin isoforms, whereas expression of filamin C is restricted to skeletal and cardiac muscle (reviewed by Van der Flier et al., 2001).

Filamin A is a dimer with two equivalent 250 kD subunits that associate with each other in a tail-to-tail, non-covalent way at their C-termini, resulting in a V-shape (Van der Flier et al., 2001). It has two N-terminal actin binding domains per dimer (see fig. 7). Most of the protein (90%) is a semi-flexible rod composed of 24 tandem repeats, each containing 96 amino acids. Its amino acid sequence predicts stretches of anti-parallel β–sheets (Yamazaki et al., 2002).

Actin fibers can be assembled in several ways, i.e. into tight parallel bundles, into loose contractile bundles, into a 70° branching network (by the Arp2/3 complex), or into a three-dimensional orthogonal network as filamins do (Stossel et al., 2001). Filamin A (FLNa) is the most potent actin-filament cross-linking protein.

Filamins bind various other macromolecules in addition to filamentous actin (see Tab. 3). A common theme among filamin-molecule interactions is the inter-webbing of the actin network with membrane receptors (see fig. 6). This is a way to provide both mechanical stability to the cell membrane and to maintain cell-cell and cell-matrix connections. Filamins thus facilitate the activation of local processes such as actin polymerization in response to signaling cascades (Stossel et al, 2001).

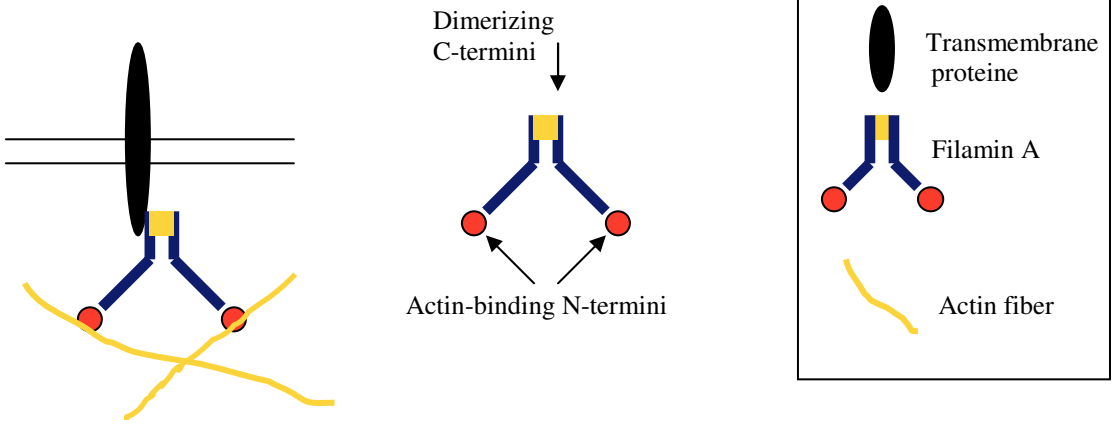

Fig. 6: Filamin A links the actin cytoskeleton with the plasma membrane via its association with integral membrane proteins

Since there is no basic homology between the binding domains that associate with the same or different filamin repeats, it remains to be resolved what determines the specificity of these interactions (Van der Flier et al., 2001). The manner in which the interaction of filamin with actin and transmembrane proteins are regulated is largely unknown. Receptor occupancy has been reported to influence the association of filamins with transmembrane receptors, this mechanism plays a role in the regulation of FcγRI receptor (Van der Flier et al., 2001). Phosphorylation of both filamin and its binding partners seems to also influence interaction. Examples of kinases that phosphorylate filamins are cAMP-kinase, PKC, and CaM-kinase II. Furthermore, tissue factor and dopamine D2 receptor reacted to phosphorylation of their cytoplasmatic tails with increase or diminish of interaction, respectively (Van der Flier et al., 2001).

Filamins are also highly susceptible to proteolysis. Calpain-mediated proteolysis results in a formation of a 240 kD amino-terminal fragment and a 10 kD carboxy-terminal fragment, causing the disruption of the actin cross-linking activity of filamin.

There is ample evidence suggesting that the proteolysis of filamin is regulated by its phosphorylation, i.e. phosphorylation modulates susceptibility for calpain-cleavage (Van der Flier et al., 2001).

Localized mutations in FLNA that conserve the reading frame lead to a broad range of congenital malformations, including craniofacial structures, skeleton, brain, viscera, and the urogenital tract. (Robertson et al., 2003).

Filamin A-associated Proteins

Membrane Proteins	*Signaling Proteins*
GP-Ibα	RalA, RhoA, Racl, Cdc42
β1A, β1D, β2, β3, β7 integrins	SEK1 (MEKK, JNKK)
FcγRI	TRAF2
Tissue factor	Trio
Dopamine D2, D3 receptor	Androgen receptor
Presenilin1, 2	
Furin receptor	*Others*
Calveolin1	
Potassium channel 4.2	FAP52
Glutamate receptor 7	CvHSP
Calcium-sensing receptor	Granzyme B
χ,δ-Sarcoglycan	BRCA2
Toll-receptor	FATZ
	Myotilin

Table 3: Filamin A associated proteins. (Taken from "Mechanical response of single filamin A molecules and its role in the actin cytoskeleton",Yamazaki et al., 2002)

One example is the genetic disorder of periventricular heterotopia (Fox et al., 1998). Periventricular heterotopia is characterized by a failure of a subset of neurons to migrate from the periventricular region to the cerebral cortex during corticogenesis, resulting in nodules of neurons, referred to as heterotopia, that are abnormally located along the ventricle.

Individuals with periventricular heterotopia usually present seizures, though the overlying cortex is often well-preserved and intelligence is often normal.

Mutations in the X-linked filamin A gene cause periventricular nodular heterotopia in males as well as in females (Robertson et al., 2003). These mutations have gain-of-function effects, implicating that filamin A is required to signal pathways that mediate organogenesis in multiple systems during neuronal migration and embryonic development.

6.0 Filamin A Interacting Protein (FILIP)

Filamin A interacting protein (FILIP) was first described by Nagano et al. in 2002.
It is a cytosolic protein with a proposed function to negatively regulate the polymerization of filamin A (Nagano et al., 2002). When FILIP is overexpressed in explants, neurons fail to migrate altogether, suggesting a role in the regulation of cortical cell migration.
In Situ hybridization of rat embryonic day 11/12 and 18/20 displayed gene expression in the ventricular zone of the cerebral cortex and in the superior colliculus, as well as gene expression in muscular tissue, including the cardiovascular system (Nagano et al., 2002).
Differential display using mRNA of the neocortices of rats showed dominant expression of FILIP mRNA at embryonic day 12, compared to significantly lower expression at embryonic day 20. At E11/E12, post-mitotic neurons are just about to migrate out of the ventricular zone towards the pial surface, suggesting that abundant FILIP expression at that state tethers cells in situ until the appropriate start of migration.
It was also reported that at E20, when neurogenesis is complete, the expression of FILIP is reduced suggesting that FILIP seems to no longer be required to control cell migration (Nagano et al., 2002).
Furthermore, Nagano et al. characterize two forms of FILIP, differing only in their 5´termini: S-FILIP (short-FILIP) lacks the 247 amino-terminal residue of L-FILIP (long-FILIP). Four leucine zipper motifs and a coiled-coil region were identified in the N-terminal half. Aside from this motif, no other signaling or transmembrane domains have been identified within FILIP.
The inhibitory effect of FILIP on filamin A, resulting in reduced cell motility, could be due to a degradation process induced by FILIP. Calpeptin-sensitive proteases such as calpain have been found to be activated by FILIP and successively to be capable of degrading filamin A (Nagano et al., 2002). F-actin associated filamin A is preferably degraded compared to actin-free filamin A.

Assays investigating the intracellular localization of GFP tagged FILIP in COS-7 cells reveal two distinct localization patterns of the two splice variants. S-FILIP and, to a very small extent, L-FILIP localizes along actin fibers, suggesting co-localization of the short iso-form with fiber-like actin. In contrast, L-FILIP is distributed in a punctuate pattern in the cytoplasma, showing no or little co-localization with fiber-like actin (Nagano et al., 2002). Furthermore, in cells expressing L-FILIP, actin stress fibers were reduced in number. This suggests that S-FILIP possesses a weaker filamin A degradation capacity and cannot completely degrade actin-networks, resulting in a fiber-like distribution along existing actin-networks. L-FILIP on the opposite strongly activates filamin A degradation processes so that no active actin networks remain in the cell and cell motility is inhibited (Nagano et al., 2002).

Among the group of filamin binding partners (see tab. 3), FILIP is unique with regard to its negative regulation of filamin A (Nagano et al., 2002).

Using the Kir3.2 C-terminus as bait in the Yeast-Two-Hybrid-System, our lab has isolated FILIP as a putative interaction partner for Kir3.2 (Delling, M., personal message, 2003). FILIP specifically binds a NSFHETYETSTPSL motif in the Kir3.2 C-terminus which is also present in other Kir channels. This motif contains tyrosine residues which can be phosphorylated. Simulating this phosphorylation *in vitro* abolishes Kir3.2/ FILIP interaction (Delling, M., personal message, 2003). Co-localization studies have also shown that FILIP co-localizes with Kir3.2 in transfected CHO cells (Delling, M., personal message, 2003). Other putative binding partners of FILIP or a physiological relevance for the interaction described above have yet to be elucidated.

III. MATERIAL

1.0 Chemicals

All chemicals were obtained from the following companies in p.a. quality:
GibcoBRL (Life technologies, Karlsruhe, Germany), Macherey-Nagel (Düren, Germany), Merck (Darmstadt, Germany), Serva (Heidelberg, Germany) and Sigma-Aldrich (Deisenhofen, Germany).
Restriction enzymes were obtained from New England biolabs (Frankfurt am Main, Germany) and MBI Fermentas (St.Leon-Rot, Germany). Molecular weight standards were obtained from Gibco.
DNA Purification Kits were purchased from Macherey-Nagel and Qiagen (Hilden, Germany).
Plasmids and molecular cloning reagents were obtained from Clontech (Heidelberg, Germany), Invitrogen (Groningen, Netherlands), Pharmacia Biotech (Freiburg, Germany), Promega (Mannheim, Germany), Qiagen and Stratagene (La Jolla, USA). All plasmids used are listed in the appendix.
Oligonucleotides were ordered from Metabion (Munich, Germany). All oligonucleotides used are listed in the appendix.
Radioactive material was ordered from Amersham Biosciences (Braunschweig, Germany).

2.0 Solutions and Buffers

(in alphabetical order)

Acetylation buffer *(In Situ Hybridization)*	0.1 0.9 2.5	M % ml/L	Triethanolamin NaCl Acetic anhydride, pH 7-8
Blocking buffer *(Immunohistochemistry)*	5 0.02	% v/v % w/v	normal goat or donkey serum sodium azide in PBS

Blocking buffer *(Western Blot)*		1-4	%(w/v)	Instant milk powder in TBS
	or	1	%(v/v)	Block solution in TBS (Boehringer)
Blotting buffer *(Western Blot)*		25	mM	Tris
		192	mM	Glycin
Boston buffer *(lysis of Bacteria)*		50	mM	Tris, pH 8.0
		1	%(w/v)	Triton X-100
		50	mM	KCl
		2.5	mM	EDTA
Denhardt's (100x) *(In Situ Hybridization)*		2	%	Ficoll
		2	%	Polyvinyl-pyrrolidone
		2	%	BSA
		ad. to 100 ml		ddH_2O
DNA-sample buffer (5x) *(DNA-gels)*		20	%(w/v)	Glycerol in TAE buffer
		0.025	%(w/v)	Orange G
dNTP stock solutions *(PCR)*		20	mM	each dATP, dCTP, dGTP, dTTP
Ethidiumbromide-staining solution		10	µg/ml	Ethidiumbromide in 1x TAE
Fixation buffer *(Immunohistochemistry)*		4	%	Formaldehyde
		0.1	%	$CaCl_2$
		0.1	M	Cycodylate buffer pH 7.3
Hybridization buffer *(In Situ Hybridization)*		50	%	Formamide
		5x		Hybridization salts (20x)
		5x		Denhardt's (100x)
		0.2	%	SDS (10%)
		10	mM	DDT
		10	%	Dextrane sulfate
		250	µg/ml	Herring sperm DNA
		250	µg/ml	Yeast tRNA

Hybridization salts (20x) *(In Situ Hybridization)*	3 0.1 0.1 ad. to 100 ml	M M M	NaCL PIPES EDTA ddH_2O
Hypotonic lysis buffer *(cell lysis)*	10 0.5	mM mM	HEPES, pH 7.4 EDTA
Ligation buffer (10x) *(DNA ligation)*	200 100 100 6	mM mM mM mM	Tris-HCL ph 7.9 $MgCl_2$ DTT ATP
Native lysis buffer *(bacterial lysis)*	50 300 10	mM mM mM	Na_2PO_4 pH 8.0 NaCl Imidazol
Paraformaldehyde (4%) *(In Situ Hybridization)*	10 1 1 25 250	g ml ml ml ml	Paraformaldehyde 10N NaOH 37% HCL 10x PBS ddH_2O
Phosphate buffered saline (PBS)	150 20	mM mM	NaCl Na_3PO_4 pH 7.4
Protease inhibitors	COMPLETE™ pills, re-suspending 1 tablet in 2ml solution results in a 25x stock solution		
RIPA buffer *(cell lysis)*	50 1 150 1 1	mM %(w/v) mM mM mM	Tris-HCL pH 7.4 Triton X-100 NaCl EDTA Na_3VO_4
Running gel *(protein gels)*	10% (8%)3.92ml(4.89ml) 5.26 ml(5.26ml) 0.14 ml(0.14ml) 4.70 ml(3.73ml) 70.0 µl(70.0µl) 7.00 µl(7.0µl)		deionized water 1 M Tris pH 8.8 10% SDS 30% acrylamide-Bis 29:1 10% APS TEMED

Sample buffer (5x)	0.31	M	Tris-HCL pH 6.8
(protein gels)	10	%(w/v)	SDS
	5	%(w/v)	ß-mercaptoethanol
	50	%(v/v)	glycerol
	0.13	%(w/v)	bromphenol blue
SDS running buffer (10x)	0.25	M	Tris-HCL pH 8.3
(protein gels)	1.92	M	glycin
	1	M	SDS
SSC (20x)	175.3	g	NaCl
(In Situ Hybridization)	88.2	g	NaCitrate, pH 7.0
Stacking gel 5%	3.77	ml	deionized water
(protein gels)	0.32	ml	1 M Tris pH 6.8
	0.05	ml	10% SDS
	0.83	ml	30% acrylamide-Bis 29:1
	25.0	µl	10% APS
	7.00	µl	TEMED
Staining solution	40	%(v/v)	ethanol
(protein gels)	10	%(v/v)	acetic acid
	0.1	%(v/v)	Serva Blue R250
Stripping buffer	0.5	M	NaCL
(Western blot)	0.5	M	acetic acid
TAE buffer (50x)	2	M	Tris-acetate pH 8.0
(DNA gel)	100	mM	EDTA
TE (10x)	0.1	M	Tris-HCL pH 7.5
	10	mM	EDTA
Tris buffered saline (TBS)	10	mM	Tris-HCL pH 8.0
	150	mM	NaCl

3.0 Bacterial Media

(in alphabetical order)

Media were autoclaved and antibiotics were supplemented prior to use.

LB-medium	10	g/l	Bactotryptone pH 7.4
	10	g/l	NaCL
	5	g/l	yeast extract
LB/ Amp-medium	100	mg/l	ampicillin in LB medium
LB/ Amp-plates	20	g/l	agar in LB medium
	100	mg/l	ampicillin

4.0 Bacterial Strains

Escherichia coli DH5α NEB

5.0 Molecular Weight Standards

1 kb DNA ladder 14 bands within the range from 200-10000bp (Gibco)

BenchMark™ 6 µl of BenchMark Prestained Protein ladder (Life Technologies) were loaded on the SDS PAGE gel:

Band no.	apparent molecular weight (kDa)
1	195.9
2	125.6
3	89.4
4	64.9 (orientation band in pink)
5	52.8
6	39.8
7	27.7
8	21.8
9	16.2
10	9.0

6.0 Plasmids

pGEM™-Easy	plasmid used for cloning and blue/white selection for recombinants on Amp-plates (Promega).

7.0 Antibodies

7.1. Primary Antibodies

anti-FILIP	Polyclonal rabbit antibody (produced in the lab of M. Sato, Tokyo). IB: 1:700 IH: 1:100
anti Kir3.2	Polyclonal rabbit antibody (produced in the lab of R.Veh, Berlin) IB 1:700 IH: 1:100
anti-MUPP1	Polyclonal rabbit antibody (produced in the lab of Y. Hamazaki, Kyoto and in the lab of K.Richter, Hamburg). IB: 1:700 IH: 1:100

7.2 Secondary Antibodies

All horseradish-coupled secondary antibodies were purchased from dianova (Hamburg, Germany) and used in a dilution of 1:10000.
For Immunohistochemistry, Cy3 and Cy5-labelled secondary antibodies were obtained from dianova and used in a dilution of 1:1000.

IV. METHODS

1.0 DNA Techniques

1.1 Maintenance of Bacterial Strains
(Sambrook et al., 1989)

Strains were stored as glycerol stocks (LB medium, 25% (v/v) glycerol) at –70°C.
An aliquot of the stock was streaked on an LB/ Amp-plate and incubated overnight at 37°C. Plates were stored for up to 6 weeks at 4°C.

1.2 Production of Competent Bacteria
(Inoue et al., 1990)

DH5α bacteria were streaked on LB-plates and grown overnight at 37°C. 50ml of LB medium was inoculated with 5 colonies and grown at 37°C until the culture had reached an optical density (OD_{600}) of 0.3-0.5.

1.3 Transformation of Bacteria
(Sambrook et al., 1989)

Either 50-100ng of plasmid DNA or 20µl of ligation mixture were added and incubated for 30 min. on ice to 100µl of competent DH5α. After a heat shock (90 sec., 42°C) and successive incubation on ice (3min.). 800µl of LB medium were added to the bacteria and incubated at 37°C for 30 min. Cells were then centrifuged (10000x g, 1min., RT) and the supernatant removed. Cells were re-suspended in 100µl LB medium and plated out on LB/amp-plates. Plates were incubated at 37°C overnight.

1.4 Plasmid Isolation from 3 ml Cultures (Minipreps)
(see Qiagen Miniprep kit)

3ml LB/amp medium (100µg/ml ampicillin) were inoculated with a single colony and incubated overnight at 37°C with constant agitation. Cultures were transferred into 2 ml Eppendorf tubes and cells were pelleted by centrifugation (12000 rpm, 1min., RT).

Plasmids were isolated from the bacteria according to the manufacturer's protocol. The DNA was eluted from the columns by addition of 50µl Tris-HCL (10mM pH 8.0) with subsequent centrifugation (12000 rpm, 2 min., RT).

1.5 Plasmid Isolation from 15 ml Cultures (Midipreps)

(see Macherey-Nagel Nucleospin kit)

The Macherey-Nagel Nucleospin kit was used in order to obtain higher amounts of DNA rapidly. 15 ml LB/amp medium (100µg/ml ampicillin) were inoculated with a single colony and incubated overnight at 37°C with constant agitation. Cultures were transferred into 15 ml Falcon tubes and cells were pelleted by centrifugation (12000 rpm, 1 min., RT) in an Eppendorf centrifuge. Plasmids were isolated from the bacteria according to the manufacturer's protocol with the following exception: the suggested amount of buffers was used twice. DNA was eluted from the columns by adding 50µl of pre-warmed (70°C) Tris-HCL (10mM pH 8.0) twice with subsequent centrifugation (12000 rpm, 2 min., RT). Then, the concentration was determined.

1.6 Enzymatic Digestion of DNA

(Sambrook et al., 1989)

The DNA was incubated with twice the recommended amount of appropriate enzymes in the recommended buffer for 2h for restriction digestions.
Restriction was terminated by addition of sample buffer and loading on an agarose gel.

1.7 Ligation of DNA Fragments

(Sambrook et al., 1989)

Ligation of DNA fragments was performed by mixing 50ng pGEMTeasy vector DNA with the 5-fold molar excess of insert DNA. 1µl of T4-ligase and 2µl of ligation buffer were added and the reaction mix was topped with deionized water to a final volume of 20µl. The reaction was incubated for 2h at room temperature. The reaction mix was used directly for transformation without any further purification.

1.8 Polymerase Chain Reaction (PCR)

(Saiki et al., 1988)

Amplifications of DNA fragments were performed in a 50µl reaction mix with thin-walled PCR tubes in MWG-PCR cyclers. *Taq*-Polymerase and the appropriate reaction buffer were obtained from Stratagene. The following reaction mixture was used:

Template	2µl
Primer up (10pM)	1µl
Primer down (10pM)	1µl
Nucleotides (dNTP, 20mM)	2µl
PCR buffer (10x)	10µl
Taq-Polymerase	0.5µl
ddH_2O	top up to 100µl

The PCR was performed with the following step gradient (touchdown PCR):

1.	Initial denaturing	95°C	5 min.
2.	Denaturing	95°C	30 sec.
3.	Annealing	58°C	30 sec.
4.	Synthesis	72°C	1 min.

The amplification procedure (steps 2-4) was repeated twice.

2.	Denaturing	95°C	30 sec.
3.	Annealing	56°C	30 sec.
4.	Synthesis	72°C	1 min.

The amplification procedure (steps 2-4) was repeated twice.

2.	Denaturing	95°C	30 sec.
3.	Annealing	54°C	30 sec.
4.	Synthesis	72°C	1 min.

The amplification procedure (steps 2-4) was repeated 19 times.

5.	Termination	72°C	5 min.
6.	Cooling	4°C	

The melting temperature of the primers depends on the GC content and was calculated using the following formula:

$$T_m = 4x\ (G+C) + 2x\ (A+T)$$

If two primers had different melting temperatures, the lower one of both was used. The quality of the PCR product was then monitored by gel electrophoresis and the PCR product was purified with the rapid PCR purification kit (Qiagen) according to the manufacturer's protocol.

1.9 DNA Gel-Electrophoresis

(Sambrook et al., 1989)

DNA fragments were separated by horizontal electrophoresis chambers (BioRad) using agarose gels. Agarose gels were prepared by heating 1-2 %(w/v) agarose (Gibco) in 1x TAE buffer, depending on the size of DNA fragments. The gel was covered with 1x TAE buffer and the DNA samples were pipetted in the sample pockets. DNA sample buffer was added to the probes and the gel was run at constant voltage (10V/cm gel length) until the orange G dye had reached the end of the gel. Afterwards, the gel was stained in an ethidiumbromide staining solution for 20 min. Then the gels were documented using the E.A.S.Y. UV light documentation system (Herolab, Wiesloh, Germany).

1.10 Extraction of DNA Fragments from Agarose Gels

(Rapid gel extraction kit, Life technologies)

For isolation and purification of DNA fragments from agarose gels, ethidiumbromide stained gels were illuminated with UV light and the appropriate DNA band was excised from the gel with a clean scalpel and transferred into an Eppendorf tube. The fragment was isolated according to the manufacturer's protocol. The fragment was eluted from the column by addition of 50µl pre-warmed (70°C) Tris-HCL (10mM pH 8.0). The concentration was determined using the undiluted eluate.

1.11 Purification of DNA Fragments

(Rapid PCR Purification kit, Life technologies)

For purification of DNA fragments, the Rapid PCR Purification kit was used according to the manufacturer's protocol. The DNA was eluted from the column by addition of 50µl pre-warmed (70°C) Tris-HCL (10mM pH 8.0). The concentration was determined using the undiluted eluate.

1.12 Determination of DNA Concentrations

DNA concentrations were determined spectroscopically using an Amersham-Pharmacia spectrometer. The absolute volume necessary for measurement was 50µl. For determining the concentration of DNA preparations, the eluate was diluted 1:50 with water and the solution was pipetted into a 50µl cuvette. Concentrations were determined by measuring the absorbance at 260nm, 280nm, and 320nm. For reliable determinations, the absorbance at 260nm had to be higher than 0.1 but lower than 0.6. A ratio of A_{260}/A_{280} between 1.8 and 2.0 monitored a sufficient purity of the DNA preparation.

1.13 DNA Sequencing

(step-by-step protocols for DNA sequencing with Sequenase-Version 2.0, 5th Edition, USB, 1990)

DNA sequencing was performed by the sequencing facility of the ZMNH. For preparation, 1µg of DNA was diluted in 7µl ddH_2O and 1µl of the appropriate sequencing primer (10mM) was added.

2.0 RNA Techniques

All materials used for handling mRNA were autoclaved. ddH_2O was stirred overnight with 0.01% diethyl-pyrocarbonate (DPEC) and was autoclaved afterwards. Glassware was baked at 180° for 3h.

2.1 *In Situ* Hybridization Analysis

[^{35}S] UTP-labeled cRNA probes corresponding to the FILIP and MUPP1-specific PCR fragments described in the appendix were generated from plasmid templates with the Maxiscript Kit (Ambion) according to the manufacturer's instructions.
SacII in combination with *sp6* was used to create the antisense strand; *NdeI* and *T7* were used to create the sense strand.
Kir3.2 specific oligonucleotides were labeled with [^{33}P] dATP using terminal desoxynucleotidyl-transferase (Boehringer) according to the manufacturer's protocol.

The mouse embryos and the mouse brains were frozen on dry ice and stored at –70°C. After embedding in Tissue Tec©, sagittal sections (16µm) were cut on a cryostat at –20°C and thaw-mounted on Superfrost plus slides (Menzel-Glaser, Braunschweig, Germany).
Before hybridization, the slides were fixed with 4 % paraformaldehyde in PBS for 10 min. at 4°C, washed twice with PBS for 5 min. at room temperature, acetylated for 10 min. in acetylation-buffer, dehydrated by successive incubations in 60 %, 80 %, 90 %, 95 %, and 100 % ethanol, chloroform, and 100 % ethanol for 5 min. each, and air-dried. After 3 hours of incubation with pre-hybridization solution (equivalent to hybridization buffer without dextrane sulfate and without probe) at 50°C, pre-hybridization solution was drained off and 100µl hybridization solution containing 2x 10^6 cpm of the probe were added, covered with coverslips, and incubated overnight in a moisturized chamber at 50°C.
Samples were washed three times in 4x SSC for 5 min. at room temperature, 30 min. in 0.5 M NaCl/ 10mM Tris-HCL pH 7.5/ 1mM EDTA/40µg RNase A per ml at 37°C, then washed for 30 min. in the same buffer wihout RNase A at 37°C, then washed twice in 2x SSC for 15 min. at 50°C.
Hybridization signals were detected by autography using Kodak Biomax MR films for 1-4 days. For more detailed detection of the signal, the hybridized cryosections were dipped in Kodak-NTB3 emulsion, incubated for 3 weeks, developed, and counterstained with Mayer's hemalaun reagent (Merck).

3.0 Protein Biochemical Methods

3.1 Protein Extraction

Protein extracts were prepared from snap frozen tissues. High protein concentrations were obtained by homogenization of 30 % (w/v) tissue in RIPA buffer at 4 °C. The homogenate was centrifuged at 20,000 × *g* and 4 °C for 30 min. to remove insoluble components. The protein content of the cleared supernatant was determined and appropriate amounts were subjected to Western blot analysis.

3.2 Determination of Protein Concentration

To ensure comparable protein concentrations in Western blot analysis, the protein extracts were subjected to protein concentration determination. Protein concentration was determined in 96 well plates using the Micro BCA Reagent (Pierce) according to the manufacturer's instructions.

3.3 SDS-Polyacrylamide Gel Electrophoresis

(Laemmli, 1970)

Separation of proteins was performed by means of the discontinuous SDS-polyacrylamide gel electrophoresis (SDS-PAGE) using the Mini-Protean III system (BioRad). The size of the running and stacking gels were as follows:

Running gel:	height 4.5cm, thickness 1mm
	8% or 10% acrylamide solution
Stacking gel:	height 0.8cm, thickness 1mm
	5% (v/v) acrylamide solution
	15-well combs

After complete polymerization of the gel, the chamber was assembled as described in the manufacturer's protocol. Up to 25µl sample were loaded in the pockets and the gel was run at constant 80V for 10 min. and then at 140V for the remainder. The gel was stopped when the bromphenol blue line had reached the end of the gel. Gels were then subjected to Western blotting.

3.4 Western Blot Analysis: Electrophoretic Transfer

(Towbin et al., 1979)

Proteins were transferred from the SDS-gel on a Nitrocellulose membrane (Protran Nitrocellulose BA 85, 0.45µm, Schleicher&Schuell) using a MINI TRANSBLOT apparatus (BioRad). After equilibration of the SDS-PAGE in blot buffer for 5 min., the blotting sandwich was assembled as described in the manufactures protocol. Proteins were transferred electrophoretically at 4°C in blot buffer at constant voltage (35V overnight).

The pre-stained marker BenchMark™ (Gibco) was used as a molecular weight marker and to monitor electrophoretical transfer.

3.5 Western Blot Analysis: Immunological Detection of Proteins on Nitrocellulose Membranes

(Ausrubel, 1996)

After electrophoresis transfer, the membranes were removed from the sandwiches and placed protein-binding side up in glass vessels. Membranes were washed once in TBS and incubated in 8ml blocking buffer for 1h at RT. Afterwards, the primary antibody was added in the appropriate dilution either for 2h at RT or overnight at 4°C. The primary antibody was removed by washing the membrane 5x5 min. with TBS. The appropriate secondary antibody was applied for 2h at RT. The membrane was washed again 5x5 min. with TBS and immunoreactive bands were visualized using the enhanced chemiluminescense detection system.

3.6 Western Blot Analysis: Immunological Detection using Enhanced Chemilumiescence

The antibody bound to the membrane was detected using the enhanced chemi-luminescence detection system (Pierce). The membrane was soaked for 1 min. in detection solution (1:1 mixture of solutions I and II). The solution was removed and the blot was placed between two saran wrap foils. The membrane was exposed to X-ray film (Biomax-MR, Kodak) for several different periods of time, starting with a 1 minute exposure.

4.0 Immunohistochemistry

4.1 Tissue Processing, Sectioning, and Immunofluorescence Staining

(Jiao Y, 1999)

Three 2-3 month-old female C57BL/6J mice were used for immunohistochemical analyses. The anesthetized animals (Narcoren®, Merial, Hallbergmoos, 60 mg kg^{-1} i.p.) were fixed by transcardial perfusion (rinse with physiologic saline for 60 sec followed by

fixation buffer for 15 min at room temperature, RT). Post-fixation was performed first in situ (by leaving the animals for 2 hours at room temperature) and then, after dissection of the brain, in the fixative used for perfusion containing 15% w/v sucrose (overnight, 4°C). Afterwards, tissue was infiltrated for additional 18 – 22 hours at 4°C with sucrose (15% w/v in cacodylate buffer) and frozen in 2-methy-butane (isopentane, Sigma). It was then pre-cooled to –30°C. Serial coronal sections were obtained in a cryostat (Leica CM3050, Leica Instruments, Nußloch, Germany, 25 µm section thickness) and collected on SuperFrost®Plus glass slides (Roth, Karsruhe). Immunolabeling was performed after antigen retrieval (30 min in 10 mM sodium citrate solution, pH 9.0, at 80°C, Jiao et al. 1999) and pretreatment with blocking solution. Polyclonal antibodies against FILIP, MUPP1 and Kir 3.2 were applied to the sections for three days at 4°C at optimal dilution (1:100 for all antibodies, in PBS containing 0.5% lambda-carrageenan, Sigma, and 0.02% w/v sodium azide). Following rinse in PBS (3 x 15 min at RT), the sections were overlaid with the secondary antibody (goat anti-rabbit conjugated with Cy3, Jackson ImmunoResearch, Dianova, Hamburg, in carrageenan solution) for 2 hours at RT. After a subsequent rinse in PBS counterstaining of nuclei was performed using bis-benzimide (5 µg ml^{-1}, 10 min at RT, Sigma). Finally, the sections were washed again and coverslipped with Fluoromount (Southern Biotechnology Associates, Biozol, Eching). Images were taken on a *Zeiss* (Jena, Germany) LSM510 confocal laser-scanning microscope.

5.0 Computer-based Sequence Analysis

Computer-based sequence analysis and alignments of DNA sequences and protein sequences was performed using the Lasergene programme (DNASTAR, *Inc.*, www.dnastar.com). The following databases were used: Medline-, BLASTN-, and BLASTP-Server of NCBI (National Center for Biotechnology Information, www.ncbi.nlm.nih.gov).

V. RESULTS

Using the Kir3.2 C-terminus as bait in the Yeast-Two-Hybrid-System, our lab has isolated MUPP1 and FILIP as putative interaction partners for Kir3.2. The objective of this study is to investigate the expression and distribution of MUPP1, Kir3.2 and FILIP to identify regions of co-expression on a cellular level, since co-expression in the same cell is the minimal requirement for Kir3.2/ FILIP and Kir3.2/ MUPP1 interaction.

1.0 Analysis of Kir3.2, FILIP, and MUPP1 mRNA Expression by *In Situ* Hybridization

In Situ hybridization experiments on cryosections of adult mouse brains were performed for the purpose of investigating expression and putative co-localization of Kir3.2, FILIP, and MUPP1 mRNA. Furthermore, expression of Kir3.2, FILIP, and MUPP1 mRNA on sections of complete embryos of different developmental stages was analyzed.

1.1 Expression of Kir3.2, FILIP, and MUPP1 mRNA in Adult Mouse Brain

[^{33}P]-labeled Kir3.2-specific antisense and sense (Fig. 7) oligoprobes were hybridized to sagittal brain sections of 3-month-old mice.

On X-ray films, a strong signal is detected in cerebellum, cortex, hippocampus, olfactory bulb (mitral cell layer, granular cell layer, and glomerular cell layer). A weaker signal is detected in thalamic nuclei and amygdaloid nuclei.

[^{35}S]-labeled FILIP-specific antisense and sense (data not shown) riboprobes were hybridized to sagittal brain sections of 3-month-old mice (Fig. 7).

In Situ hybridization of FILIP cRNA in adult brains reveals weak signals in the hippocampus, cerebellum, cortex, olfactory bulb, and pontine nucleus.

[^{35}S]-labeled MUPP1-specific antisense and sense (data not shown) riboprobes were hybridized to sagittal brain sections of 3-month old mice (Fig. 7).

MUPP1 mRNA is weakly expressed in adult brain, showing signals in the hippocampus, cortex, cerebellum, and pontine nuclei.

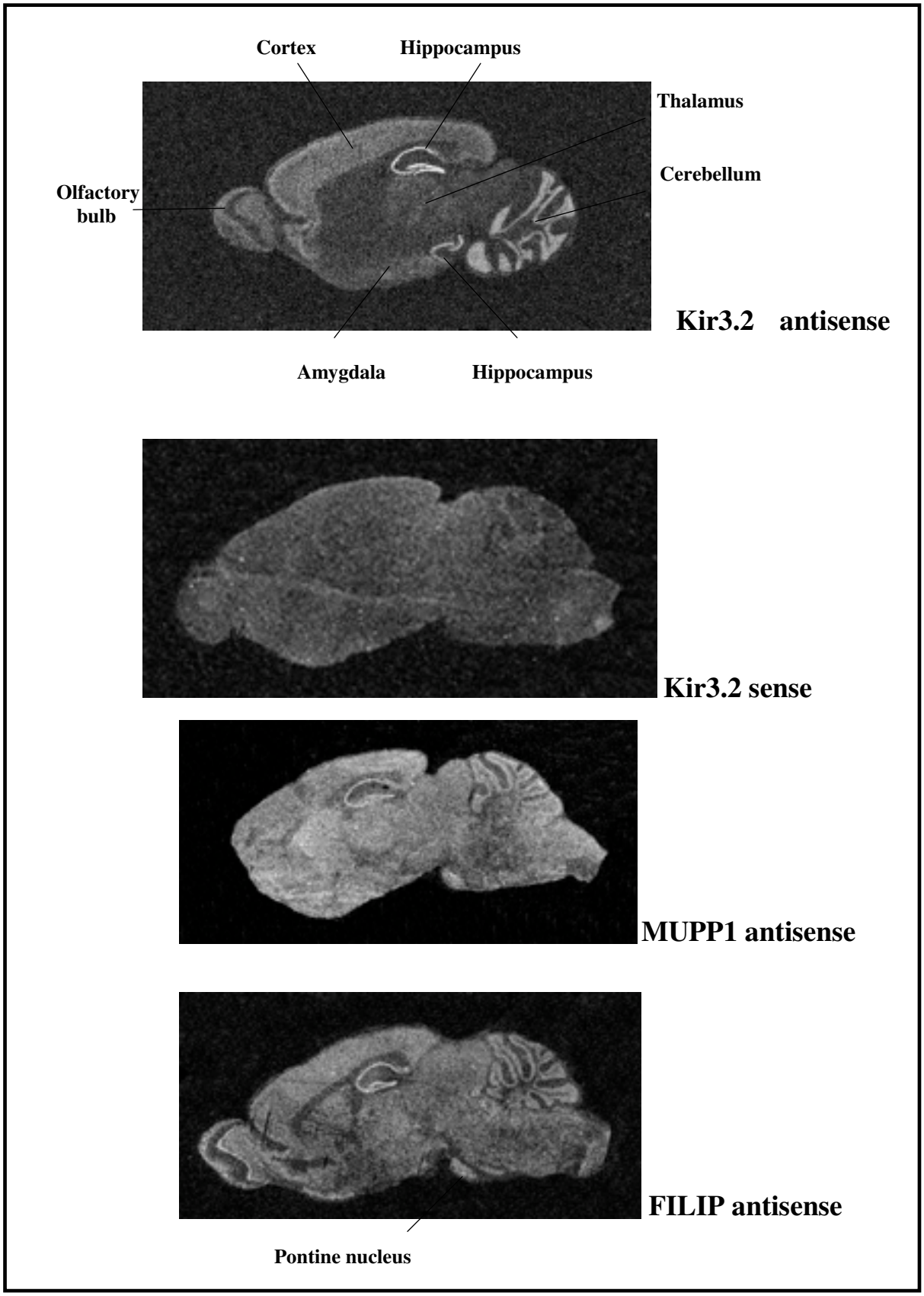

Fig. 7: Comparison of Kir3.2, FILIP, and MUPP1 mRNA expression in adult mouse brain

Kir3.2 and FILIP are both expressed in the cortex, cerebellum, hippocampus, and olfactory bulb (see Chapter 3.0 "Immunohistochemistry of Kir3.2 and FILIP Protein Expression in Adult Mouse Brain" for further reference).
Kir3.2 and MUPP1 are also both expressed in the cortex, cerebellum, and hippocampus. The olfactory bulb is not visible on the cryostat section presented.

1.2 Expression of Kir3.2, FILIP, and MUPP1 mRNA at different Developmental Stages

- **E14:** [^{35}S]-labeled FILIP-specific antisense and sense (data not shown) riboprobes were hybridized to sagittal sections of embryos day E14 (Fig. 8).
  Signal detection in E14 reveals FILIP mRNA in the cortex and superior colliculus.
  [^{35}S]-labeled MUPP1-specific antisense and sense (data not shown) riboprobes were hybridized to sagittal sections of embryos day E14 (Fig. 8).
  In E14, weak hybridization signals were found in the superior colliculus, cortex, medulla, and spinal cord.
- **E16:** [^{33}P]-labeled Kir3.2-specific antisense and sense (data not shown) oligoprobes were hybridized to sagittal sections of embryos day E16 (Fig. 9).
  Kir3.2 mRNA expression on day 16 shows a strong signal in spinal cord and dorsal root ganglia. In brain, very low expression is detectable in superior colliculus, medulla, and olfactory bulb.
  [^{35}S]-labeled FILIP-specific antisense and sense (data not shown) riboprobes were hybridized to sagittal sections of embryos day E16 (Fig. 9).
  FILIP specific probe shows distinct signals in the spinal cord, dorsal root ganglia, superior colliculus, cortex, and olfactory bulb. FILIP mRNA expression was also detected in regions outside the nervous system. A FILIP specific signal was found in heart, great vessels, and gastrointestinal tract.
  [^{35}S]-labeled MUPP1 specific antisense and sense (data not shown) riboprobes were hybridized to sagittal sections of embryos day E16 (Fig. 9).
  In E16, MUPP1 mRNA is detected in the cortex, superior colliculus, olfactory bulb, medulla, and dorsal root ganglia.
  Kir3.2 and FILIP are both expressed in the spinal cord, dorsal root ganglia, superior colliculus, and olfactory bulb on embryonic day E16.

Kir3.2 and MUPP1 are both expressed in the dorsal root ganglia, superior colliculus, medulla, and olfactory bulb on embryonic day E16.

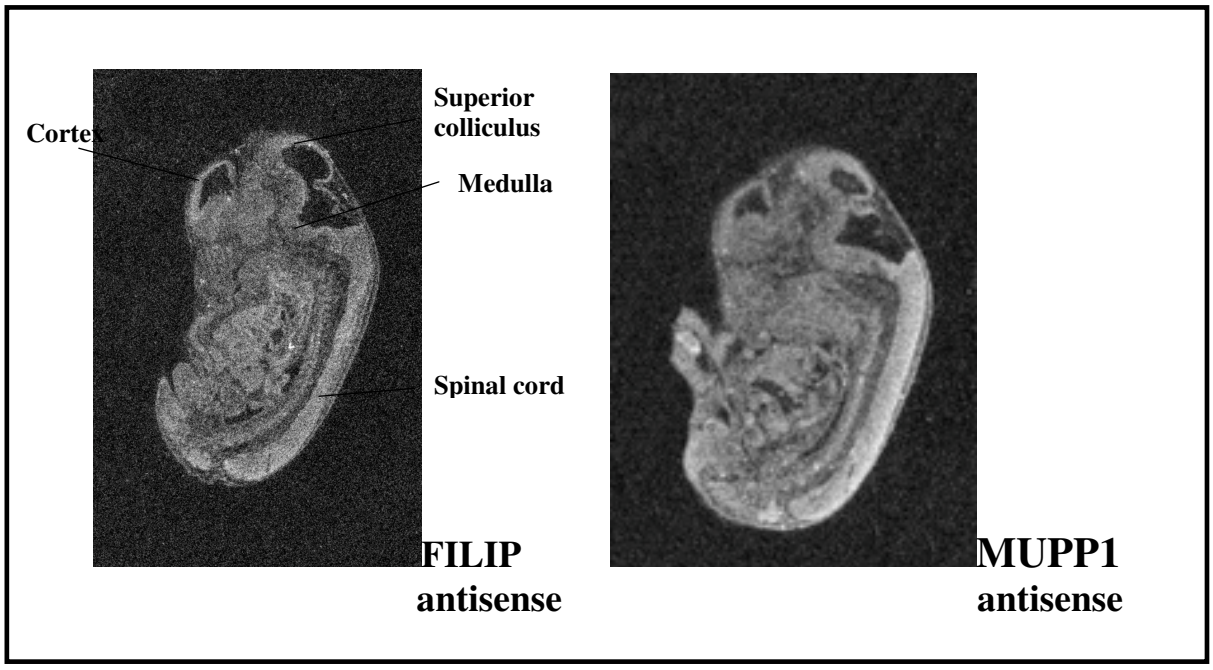

Fig. 8: Comparison of FILIP and MUPP1 mRNA expression in mouse embryonic day 14

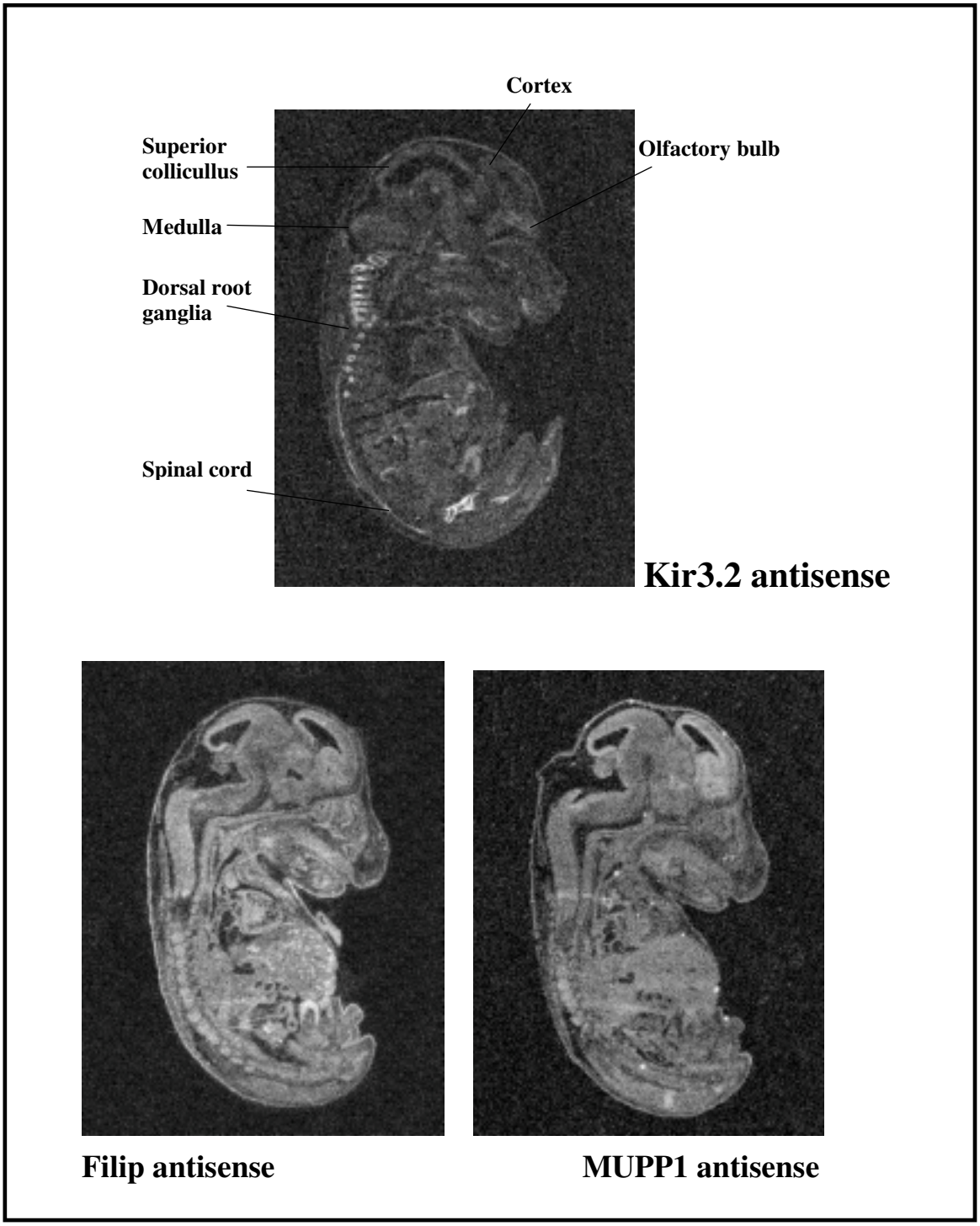

Fig. 9: Comparison of Kir3.2, FILIP, and MUPP1 mRNA expression in mouse embryonic day 16

1.3 Expression of FILIP and MUPP1 mRNA in the Hippocampus and the Cerebellum

In order to investigate FILIP and MUPP1 mRNA expression in more detail and to compare it with the immunohistochemical results, the hybridized cryosections were dipped in photographic emulsion, exposed for 3 weeks, developed, and counterstained with Mayer's hemalaun reagent.

FILIP mRNA is strongly expressed (black silvergrains) in hippocampus region CA1/3 (Fig. 10) and in the Purkinje cell layer of the cerebellum (Fig. 11).

MUPP1 mRNA is weakly expressed in the hippocampal region CA1/3 (Fig. 10) and in cerebellum (Purkinje cell layer) (Fig. 11).

Both FILIP and MUPP1 mRNA are expressed in the same cell layers - that is hippocampus region CA1/3 and cerebellum (Purkinje cell layer).

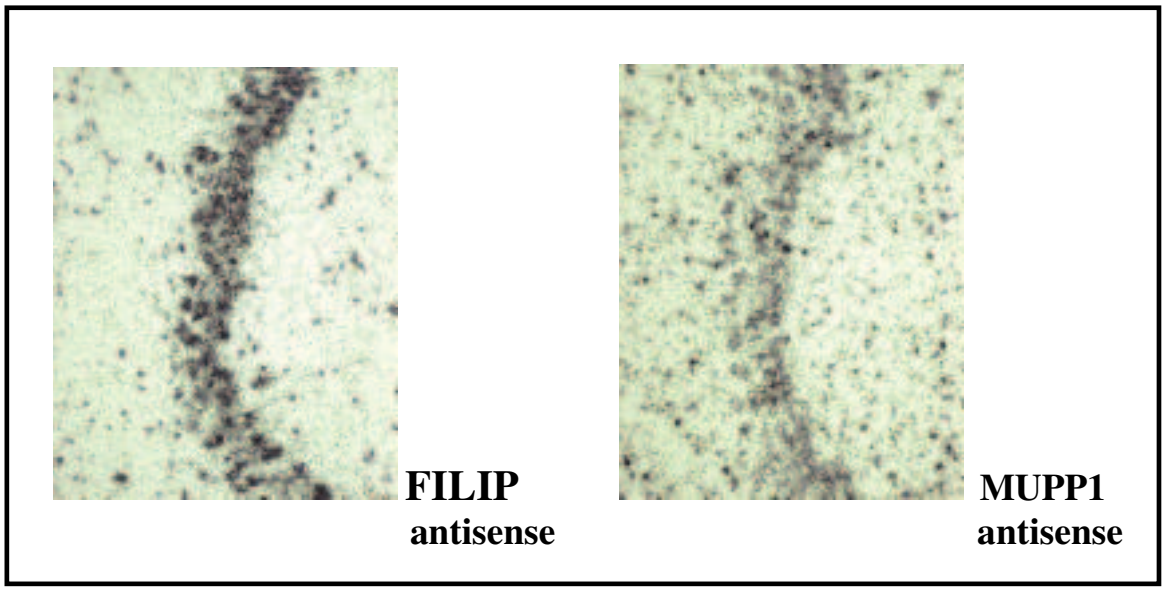

Fig. 10: Comparison of FILIP and MUPP1 mRNA expression in the hippocampal region CA 1/3 (Obj. 10x).

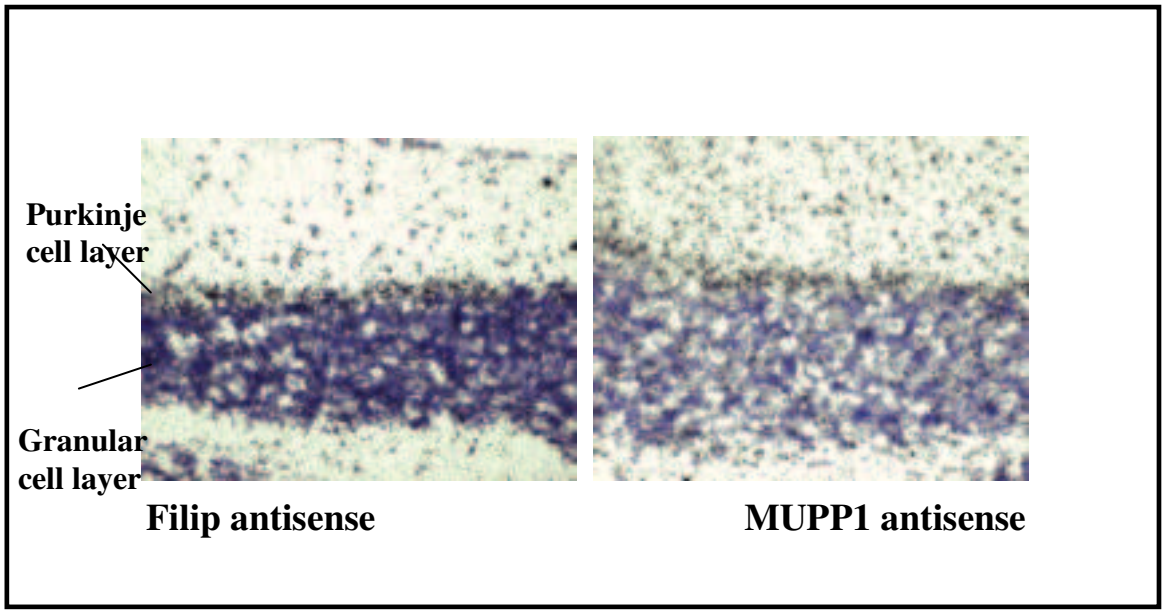

Fig. 11: Comparison of FILIP and MUPP1 mRNA expression in cerebellum (Obj.10x).

2.0 Analysis of Kir3.2, FILIP, and MUPP1 Protein Expression by Western Blot Assay

In order to investigate putative concurrence of Kir3.2, FILIP, and MUPP1 expression on protein level, immunoblot analyses of different body tissues of adult mice were performed.

Immunoblots of crude tissue extracts from different body tissues of adult mice detected a protein of approximately 55 to 60 kD (Fig. 12), which is in close accordance with the calculated molecular weight of Kir3.2, two proteins of approximately 120kD and 140 kD (Fig. 12), which is in accordance with the calculated molecular weight of the two splice forms of FILIP: S-FILIP (short FILIP) and L-FILIP (long-FILIP), respectively, and a protein of approximately 220kD (Fig. 12), which is in accordance with the calculated molecular weight of MUPP1.

The immunoblot analysis shows strongest Kir3.2 expression in the brain and the stomach and a weak signal in the heart.

The strongest expression of FILIP is found in the spleen, lung, heart, and brain.

MUPP1 reveals strongest expression in the brain, followed by heart, spinal cord, lung, and stomach. Here, signals of proteins with a lower molecular weight were also detected. One such protein had a molecular weight of approx. 100 kD in the liver, spleen, stomach, skeletal muscle, and kidney; one such protein had a molecular weight of approx. 75 kD in the stomach and kidney, as well as signals at approx. 65kD in the brain, and approx. 50 kD in the heart, spleen, and stomach.

Kir3.2 and FILIP are both strongly expressed in the brain; they are also both expressed in the heart.

Kir3.2 and MUPP1 are both strongly expressed in the brain and stomach; they are also both expressed in the heart.

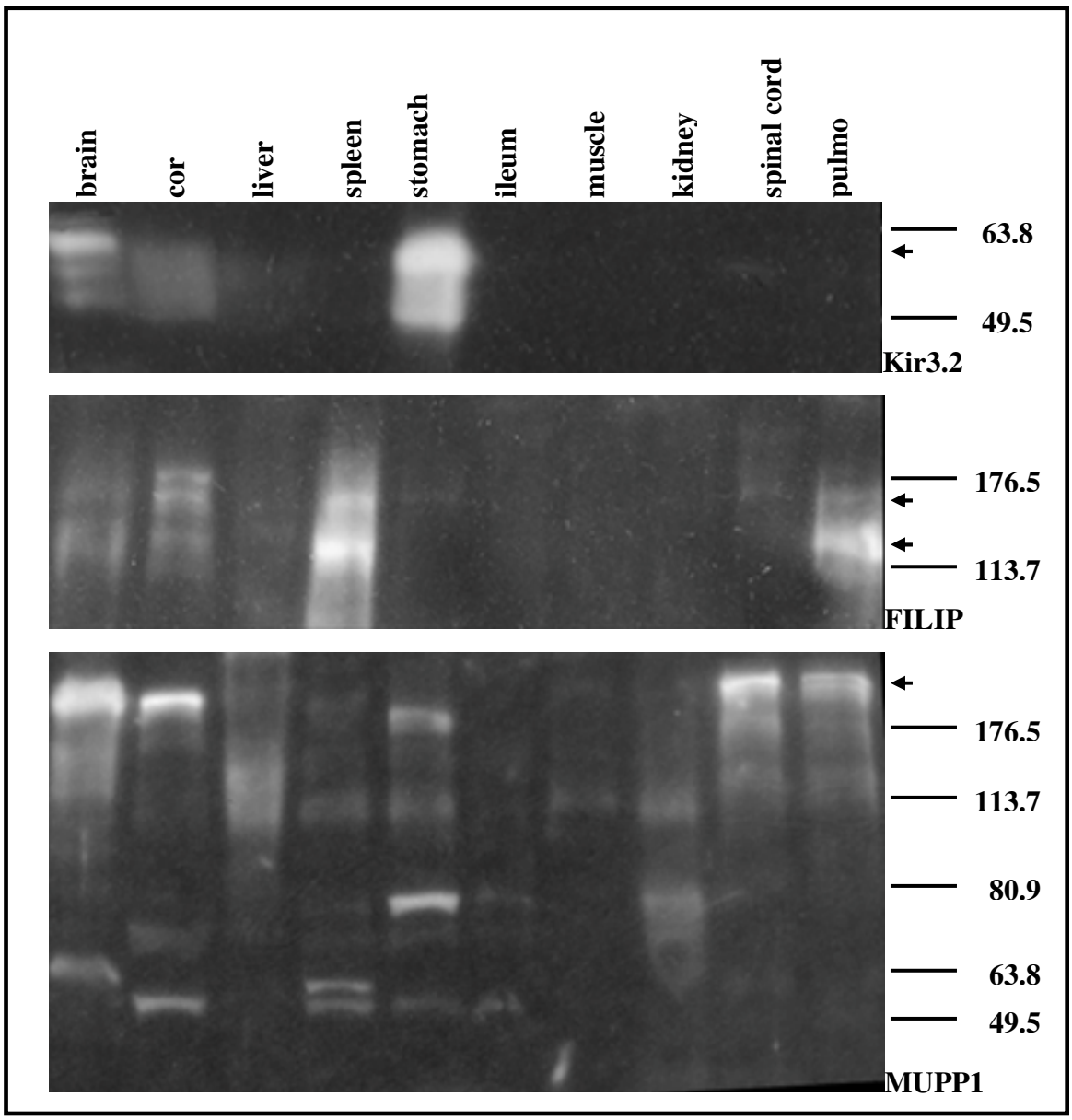

Fig. 12: Comparison of Kir 3.2, FILIP, and MUPP1 immunoblot assays

3.0 Immunohistochemistry of Kir3.2 and FILIP Protein Expression in the Adult Mouse Brain

Immunohistochemical analyses of adult mice brain were performed in order to further investigate a putative co-localization of Kir3.2 and FILIP in the central nervous system on a protein level and to add a more detailed view of certain brain areas to the *In Situ* analysis.

We focused on the Kir3.2 and FILIP co-localization, since MUPP1 Immunohistochemistry did not produce reliable results with the available MUPP1 antibody.

3.1 Immunohistochemistry Analysis of FILIP Protein Expression

Figures 14 to 18 show immunohistochemical analyses of FILIP protein expression in brain sections of adult mice.

Low magnification views (5x) show strong FILIP immunofluorescence labeling throughout the cortex and in the hippocampus (CA1-3 and gyrus dentatus) (Fig. 13).

In the cortex, cells in layers III – VI are stained (magnification 20x). Comparison of nuclear staining and immunolabeling indicates that a high proportion of all cells present in these cortical areas are positive (Fig. 14). Higher magnification views (40x) show that FILIP staining is limited to cytoplasma with additional staining in apical dendrites of presumptive pyramidal cells (Fig. 15).

In the dentate gyrus, FILIP labeling occurs in granule cell bodies and in interneurones in both molecular and polymorphic layers (Fig. 16).

In the hippocampal region CA1, FILIP signals are confined to pyramidal cell bodies and interneurones. In addition, pyramidal cell dendrites in stratum radiatum (two asterisks) but not in stratum oriens (one asterisk) are apparently stained (Fig. 17).

FILIP protein in adult mouse brain is thus found in cortex and hippocampus (CA1-3 and dentate gyrus). It is located intracellularly, in cell bodies, and in dendrites - to a lower extent.

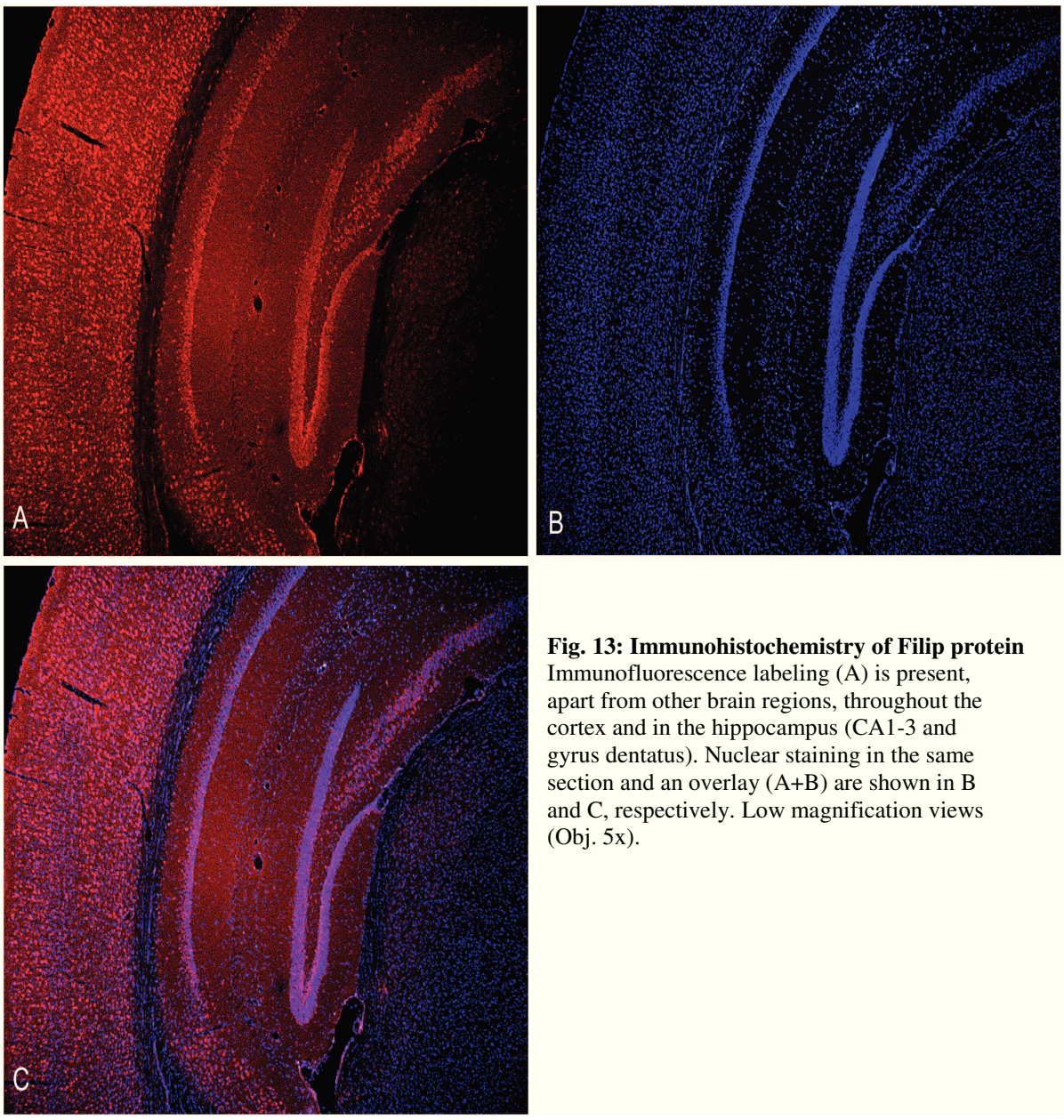

Fig. 13: Immunohistochemistry of Filip protein
Immunofluorescence labeling (A) is present, apart from other brain regions, throughout the cortex and in the hippocampus (CA1-3 and gyrus dentatus). Nuclear staining in the same section and an overlay (A+B) are shown in B and C, respectively. Low magnification views (Obj. 5x).

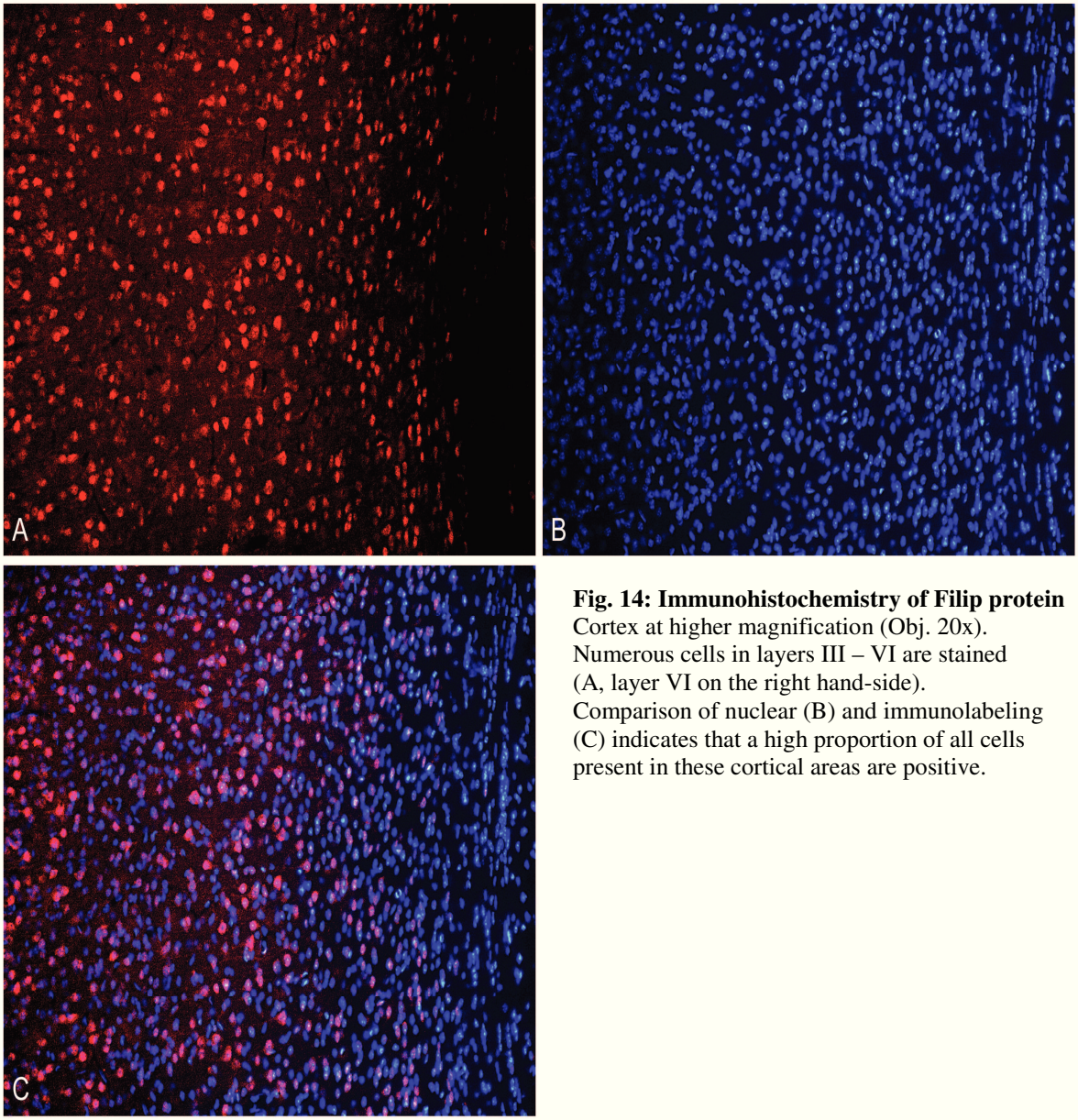

Fig. 14: Immunohistochemistry of Filip protein
Cortex at higher magnification (Obj. 20x). Numerous cells in layers III – VI are stained (A, layer VI on the right hand-side). Comparison of nuclear (B) and immunolabeling (C) indicates that a high proportion of all cells present in these cortical areas are positive.

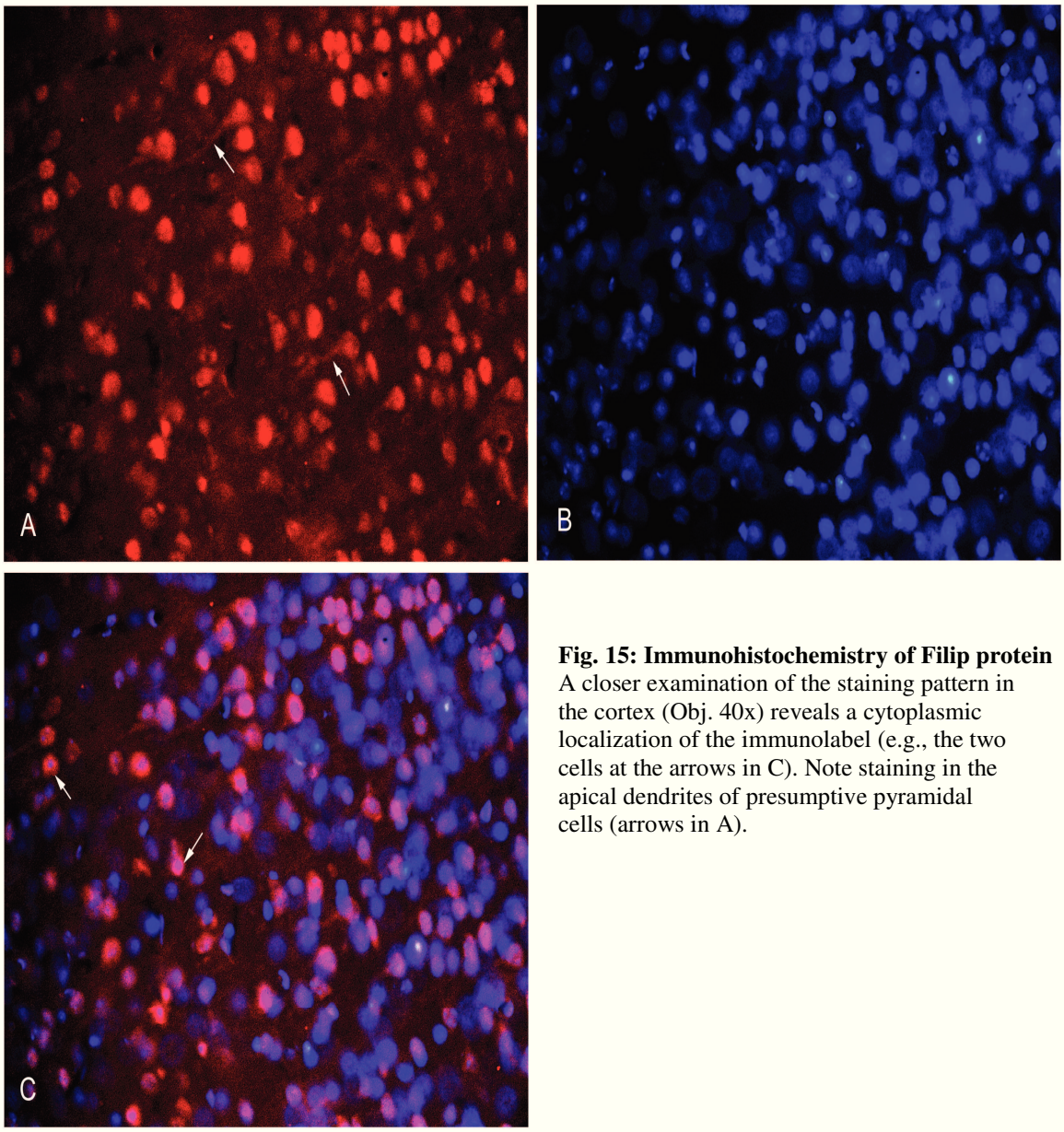

Fig. 15: Immunohistochemistry of Filip protein
A closer examination of the staining pattern in the cortex (Obj. 40x) reveals a cytoplasmic localization of the immunolabel (e.g., the two cells at the arrows in C). Note staining in the apical dendrites of presumptive pyramidal cells (arrows in A).

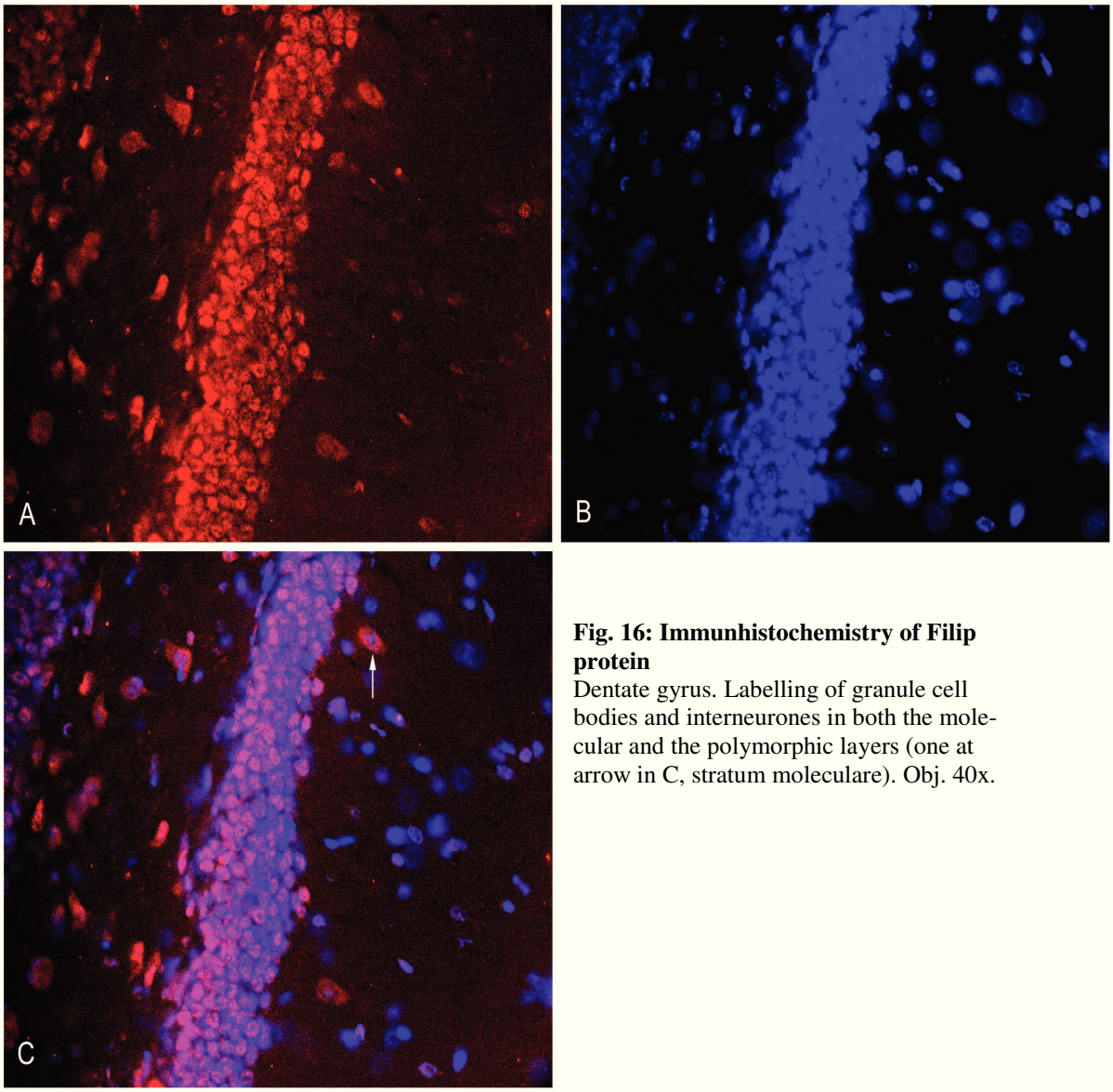

Fig. 16: Immunhistochemistry of Filip protein
Dentate gyrus. Labelling of granule cell bodies and interneurones in both the molecular and the polymorphic layers (one at arrow in C, stratum moleculare). Obj. 40x.

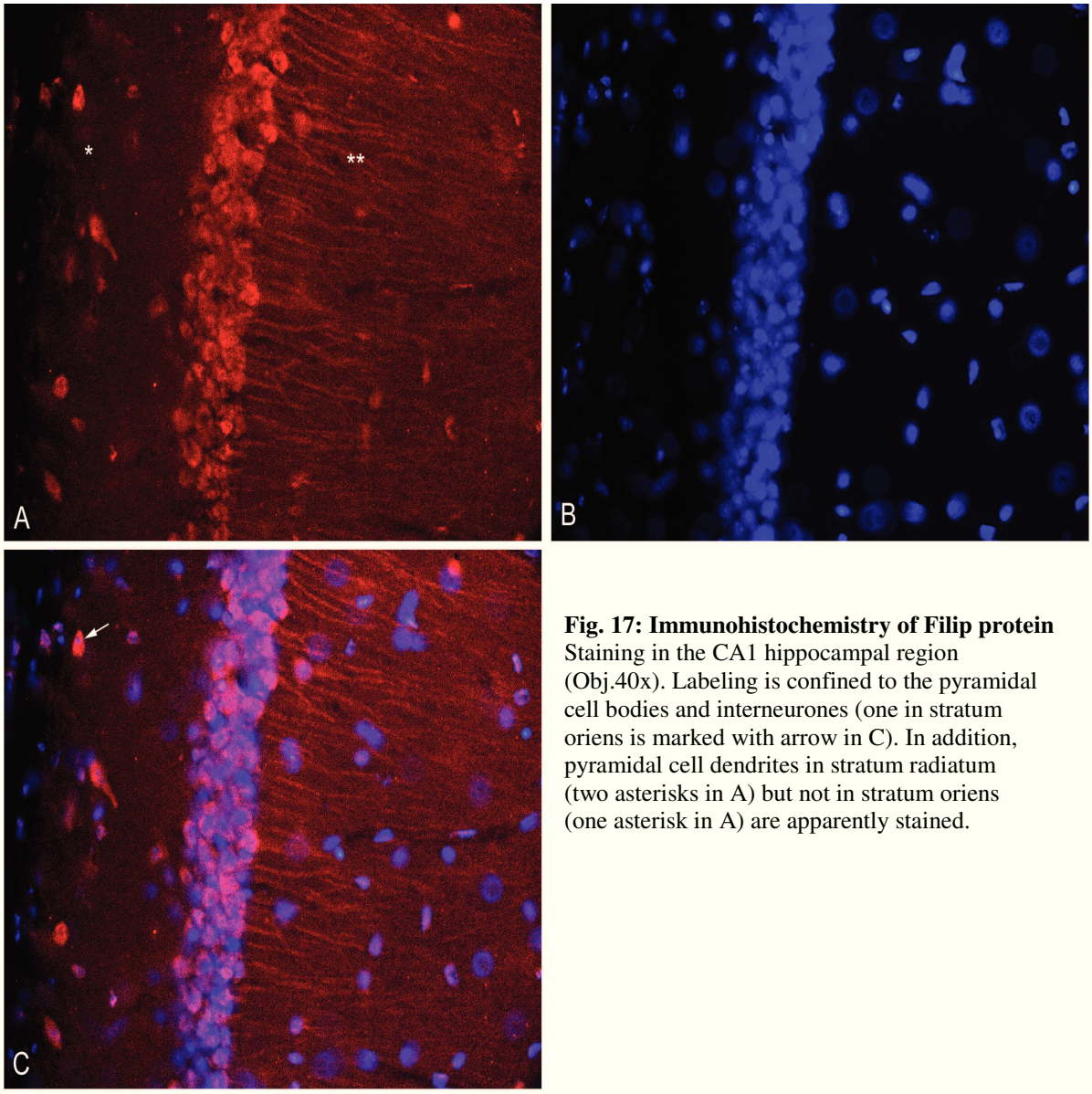

Fig. 17: Immunohistochemistry of Filip protein
Staining in the CA1 hippocampal region (Obj.40x). Labeling is confined to the pyramidal cell bodies and interneurones (one in stratum oriens is marked with arrow in C). In addition, pyramidal cell dendrites in stratum radiatum (two asterisks in A) but not in stratum oriens (one asterisk in A) are apparently stained.

3.2 Comparison of FILIP and Kir3.2 Immunohistochemistry

Figure 18 compares Kir3.2 immunostaining with FILIP immunostaining in cortex and hippocampus.

Although Kir3.2 signal is also present in cortex and hippocampus, Kir3.2 and FILIP staining patterns are not congruent, as the arrows in Figure 18 indicate.

The majority of Kir3.2 protein is not localized in the cell somata, but rather in dendrites, whereas the majority of FILIP protein is located in the somata.

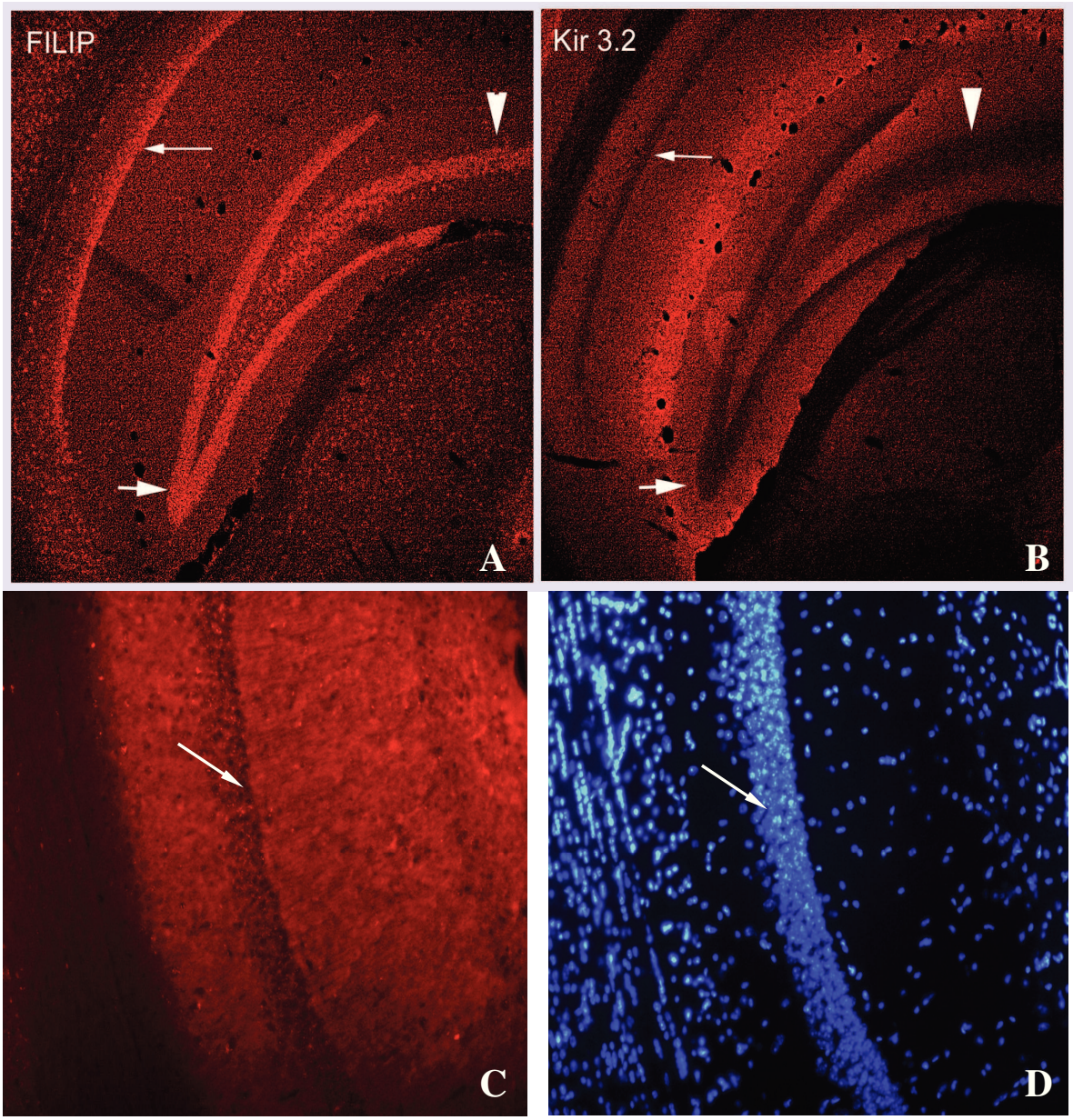

Fig. 18: Immunohistochemistry of Filip and Kir3.2 protein
Co-localization study of Filip and Kir3.2 in serial sections of mouse hippocampus (Ob. 5x) (A+B). In CA-1, the majority of Kir3.2 protein is not localized in the somata (compare C with nuclear staining in D), but rather in the dendrites (Ob. 20x).

VI. DISCUSSION

A putative concurrence of Kir3.2, FILIP, and MUPP1 mRNA and protein expression and distribution in the mouse model was investigated in the study on hand.

Previous studies have shown that the neuronal cell adhesion molecule NCAM regulates the surface delivery of Kir3.2 (Delling et al., 2002). However, the underlying mechanism of this regulation has not yet been described.

One of the likely molecular mechanisms postulates the existence of a common binding partner, shared by Kir3.2 and NCAM.

Using the Yeast Two-Hybrid screening system, two potential Kir3.2 interaction partners were identified: the Filamin A interacting protein (FILIP) and the multiple PDZ protein MUPP1 (unpublished results). Both proteins have been characterized by previous studies and will be discussed at a later stage.

Co-expression in the same cell is the minimal requirement for a putative Kir3.2/FILIP and Kir3.2/MUPP1 interaction. Therefore, Western Blot analysis, *In Situ* hybridization, and Immunohistochemistry of these three molecules was performed to narrow down the regions of putative cellular co-expression for further studies investigating the physiological role of the FILIP/Kir3.2 and MUPP1/Kir3.2 interaction.

1.0 Kir3.2, FILIP, and MUPP1 show Co-expression on mRNA Level in different Brain Regions during Embryogenesis and in the Adult Mouse Brain

- **Kir3.2:** Analysis of Kir3.2 mRNA expression in the adult mouse brain using *In Situ* hybridization reveals a Kir3.2 signal in cerebellum, cortex, hippocampus, olfactory bulb (mitral cell layer, granular cell layer, and glomerular cell layer). A weaker signal is detected in thalamic nuclei and amygdaloid nuclei.

  Kir3.2 mRNA expression analysis in the mouse brain during embryogenesis (E16) reveals a Kir3.2 signal in spinal cord, superior colliculus, medulla, olfactory bulb, and dorsal root ganglia.

  These findings are in close accordance with the results published by Karschin in 1997 (Karschin and Karschin, 1997). This group has thoroughly investigated the gene expression of Kir3.2 using *In Situ* hybridization. During embryogenesis, Kir 3.2 mRNA signal appears in the spinal cord as early as embryonic day E12.

On E13, a positive signal was found in the substanitia nigra, cerebellum, superior colliculus, pons, and in the medulla. On E15, a positive signal was detected in hippocampus and thalamus, on E17 in hypothalamus and septum and on E19 in the cortex, especially in cingulate gyrus and entorhinal cortex.

Additionally, Kir3.2 mRNA was found in the peripheral nervous system, in DRG, and in cranial sensory ganglia by E17.

- **FILIP:** Analysis of FILIP mRNA expression by *In Situ* hybridization in adult brain reveals signals in the hippocampus, cerebellum, cortex, olfactory bulb, and pontine nucleus.

  At higher magnification views, FILIP mRNA can be found in the hippocampal region CA1/3 and in cerebellum (Purkinje cell layer).

  During embryogenesis (E14 and E16), hybridization signals were detected in the cortex, superior colliculus, spinal cord, dorsal root ganglia, and olfactory bulb. Expression of FILIP mRNA was detected in several unrelated anatomical structures aside from the nervous system. A FILIP-specific signal was found in heart, great vessels, and gastrointestinal tract.

  The FILIP expression in heart, great vessels, and gastrointestinal tract found in Western Blot and *In Situ* analysis of E14 and E16 may be explained by the high sequence homology shared by Filamin C and Filamin A. Filamin C, which is predominantly found in smooth and skeletal muscular tissues, may be regulated by FILIP in these tissues in a similar way as Filamin A is regulated in the brain (Nagano et al., 2002). This would explain FILIP expression in tissues others than neuronal.

  Our observations are in agreement with the data from Nagano et al., 2002 who also performed *In Situ* analysis of FILIP mRNA expression using rat embryonic day 11/12 and 18/20.

  On embryonic day 12, this group detected a FILIP mRNA signal in the cortex and superior colliculus. On embryonic day 18, additional signals in the heart, great vessels, gastrointestinal tract, and diaphragma were found.

- **MUPP1:** The analysis of MUPP1 mRNA expression by *In Situ* hybridization reveals weak expression of MUPP1 mRNA in the adult brain, showing signals in the hippocampus, cortex, cerebellum, and pontine nuclei.

At higher magnification views, MUPP1 mRNA can be found in the hippocampal region CA1/3 and in the cerebellum (Purkinje cell layer).

During embryogenesis (E14 and E16), weak hybridization signals were found in the superior colliculus, cortex, medulla, spinal cord, olfactory bulb, and dorsal root ganglia.

Bécamel et al., 2001 and Sitek et al., 2003 also performed *In Situ* assays. They found high levels of MUPP1 in the choroid plexus, hippocampus, dentate gyrus, amygdala nuclei, pontine nuclei, piriform cortex, all neocortical layers, and in purkinje cell layer in the cerebellum.

Summarizing the given data so far, it can be assumed that Kir3.2, MUPP1 and FILIP mRNA are co-expressed in the following brain areas during embryogenesis and in the adult brain:

- during embryogenesis, Kir3.2, MUPP1 and FILIP mRNA are co-expressed in the spinal cord, dorsal root ganglia, superior colliculus, medulla, and olfactory bulb.
- in the adult, Kir3.2, MUPP1 and FILIP mRNA are co-expressed in the cortex, cerebellum (Purkinje cell layer), hippocampus region CA1/3, and olfactory bulb.

2.0 Kir3.2, FILIP, and MUPP1 show Co-expression on Protein Level in Several Tissues in the Adult Mouse

- **Kir3.2:** The immunoblot analysis shows the strongest Kir3.2 expression in the brain and stomach and a weak signal in heart.

  Karschin and Karschin (1997) described that Kir3.1, Kir3.2, and Kir3.3 subunits are abundantly expressed in several brain areas. In contrast, Kir3.4 subunits are mainly expressed in the heart and form the atrial K(Ach) channels together with the Kir3.1 subunit (Karschin and Karschin, 1997). The Kir3.1/3.2 and Kir3.1/3.3 channels are thus commonly referred to as the neuronal Kir3 channels, whereas the Kir3.1/3.4 channel is depicted as the cardiac Kir3 channel.

  The Kir3.2 protein signal found in the heart may thus be explained by a possible cross-reaction with the Kir3.1/3.4 channel abundantly expressed in the heart.

The antibody staining for Kir3.2 found in the stomach has not yet been described. Further studies are necessary to confirm the specificity of the antibody staining.

- **FILIP:** Our data show that the strongest expression of FILIP is found in the spleen, lung, heart, and brain.

  Nagano et al., 2002 investigated FILIP protein expression in the cortex only and found FILIP protein in embryos day E12, E15, E18, P0, and P7. After day P7, this group was not able to detect FILIP expression in the cortex.

  Since we did not use only the cortex but the whole brain, our assay can neither prove nor disprove these findings. Furthermore, Nagano et al did not investigate FILIP expression in other tissues.

- **MUPP1:** The Western Blot assay using anti MUPP1 antibodies reveals several proteins with different molecular weights. The MUPP1 protein of approx. 220kDa was found predominantly in the brain, heart, spinal cord, lung, and stomach; one protein with a molecular weight of approx.100 kDa was found in the liver, spleen, stomach, skeletal muscle, and kidney; one protein with a molecular weight of approx. 75 kDa was found in the stomach and kidney. More signals were detected at approx. 65 kDa in thebrain, and approx. 50 kDa in the heart, spleen, and stomach.

  These observations are in agreement with Sitek et al., 2003. This group published MUPP1 Western Blot analysis results that revealed a band at 220 kDa in the brain, skeletal muscle, heart, liver, kidney, and lung. An additional band at 50 kDa was observed in the heart and lung, two bands at 30kDa and 75kDa in the liver and one at 100kDa in the kidney.

  Ullmer et al., 1998 examined tissue distribution using Northern Blot analysis. An 8.5kb MUPP1 mRNA transcript, encoding for the complete 220kDa protein was present in the heart, brain, placenta, liver, skeletal muscle, kidney, testicles, spleen, and pancreas (Mancini et al, 2000; Ullmer et al.,1998). A 5.0kb transcript was detected in the heart, liver, and kidney, and a 4.0 kb transcript in the brain (Ullmer et al., 1998). Mancini et al. (2000) found a 7.5kb and a 5.0kb transcript in the skeletal muscle and liver, and a 1.0kb transcript in the heart, skeletal muscle and liver (Mancini et al., 2000).

These findings suggest that differential expression, alternative splicing, and/or posttranslational modification produce tissue-specific forms of MUPP1 (Mancini et al, 2000; Sitek et al.,2003; Ullmer et al., 1998). The individual splicing products that the PDZ domains are made of have not yet been identified. Other PDZ proteins, such as PDZ-73, are known to have at least five different tissue-specific splice variants (Scanlan et al., 1999).

Bécamel et al., 2001 and Sitek et al., 2003 show that *In Situ* hybridization and Immunohistochemistry reveal a similar distribution pattern for MUPP1 mRNA and protein throughout the brain. They found MUPP1 protein expression in the epithelial cells of the choroid plexus, in hippocampus CA1-4 pyramidal cells, and in stratum radiatum and stratum oriens. Furthermore, they found MUPP-1 expression in the granular cell layer of dentate gyrus and in most neocortical layers. MUPP1 protein was also found in the piriform cortex, amygdala nuclei, subiculum, olfactory bulb, cerebellum purkinje cell layer, in pontine nuclei, parts of spinal trigeminus, principal sensory trigeminus, and in all thalamic and hypothalamic nuclei and substantia nigra.

Summarizing the given data so far, it can be assumed that Kir3.2, MUPP1 and FILIP protein are present simultaneously in the brain and heart in the adult mouse.

3.0 FILIP Protein is Expressed in the Adult Mouse Brain

Since Nagano et al., 2002 did not publish any FILIP Immunohistochemistry data, our findings provide a first overview of FILIP protein expression in the adult mouse brain using immunohistochemical methods.

Low magnification views (5x) show strong FILIP immunofluorescence labeling throughout the cortex and in the hippocampus (CA1-3 and gyrus dentatus). It is located intracellularly, in cell bodies, and in dendrites - to a lower extent.

In the cortex, cells in layers III – VI are stained. A high proportion of all cells present in these cortical areas are positive.

Higher magnification views (40x) show that FILIP staining is limited to cytoplasma with additional staining in apical dendrites of presumptive pyramidal cells.

In the dentate gyrus, FILIP labeling occurs in granule cell bodies and in interneurones in both molecular and polymorphic layers. In the hippocampus region CA1, FILIP signals are confined to pyramidal cell bodies and interneurones. In addition, pyramidal cell dendrites in the stratum radiatum but not in the stratum oriens are apparently stained. The underlying reason for this distinct distribution pattern remains to be elucidated.

Nagano et al., 2002 used Western Blot and *In Situ* hybridization assays to address the question of FILIP expression and distribution. This group did not find FILIP mRNA or protein in migratory or post-migratory neurons, i.e. in adult animals.

In contrast to these results, our findings suggest that FILIP is abundantly expressed in the adult mouse brain, both on the mRNA and on the protein level, as well as in other unrelated anatomical structures.

In contrast to FILIP immunostaining, which is limited to the cytoplasma, Immunohistochemistry of Kir3.2 protein expression in the cortex and hippocampus shows that the majority of Kir3.2 protein is not localized in the cell somata, but rather in the postsynaptic densities of neurons. This localization pattern reflects the physiological role of Kir3.2 and FILIP at the cell surface of postsynaptic densities and in the cytoskeleton, respectively.

Immunohistochemistry assays of MUPP1 protein expression in the adult mouse brain did not produce reliable results. Using both the polyclonal antibodies from Hamazaki, Tokyo and from Richter, Hamburg, we were not able to produce a satisfying MUPP1 immunostaining.

Sitek et al., 2003 developed a new antibody for their assays. Using this new antibody, they were able to define MUPP1 protein expression in different brain regions (see Chapter 2.0 for details).

4.0 Putative Physiological Relevance of the Interactions Studied

This study is the first to demonstrate that the potassium channel Kir3.2 and the PDZ protein MUPP1 are co-expressed in different tissues and brain regions during embryogenesis and in the adult mouse and can thus possibly interact with each other.

PDZ domains have emerged in the past years as important protein-protein interaction modules. They are typically involved in the assembly of supramolecular complexes that perform localized signaling functions at particular subcellular locations. Organization

around a PDZ-based scaffold allows the stable localization of interacting proteins and enhances the rate and fidelity of signal transduction within the complex.

Some PDZ-containing protein may not only be involved in arranging binding partners, but also in the trafficking of interacting proteins within the cell. PSD-95 e.g. clusters glutamate receptors and K^+ channels in the postsynaptic density of excitatory synapses (Sheng et al., 2001) and Thomas et al. (1997) identified FasII, the *Drosophila* homologue of NCAM, to cluster shaker K^+ channels in the cell membrane via the intra-cellular PDZ protein discs-large (dlg).

Kim and Sheng (2004) suggest that this clustering at the cell surface may be related to inhibition of membrane internalization since e.g. removing the PSD95 binding motif from the receptor protein NR2B leads to enhanced membrane internalization (Roche et al., 2001). The same was shown for the Kv1.4 potassium channel and its PSD95 binding motif (Jugloff et al., 2000).

Since further studies were able to additionally show an interaction between MUPP1 and NCAM (Delling, personal message, 2003), we now propose that MUPP1 may present the missing link to understanding the way in which NCAM regulates cell surface localization of Kir3.2. MUPP1 as an interaction module would thus prevent Kir 3.2 membrane internalization which leads to reduced Kir3.2 channel activity during periods of NCAM protein up-regulation, such as development. This increases the impedance of postsynaptic membranes and thus neurons become more sensitive to synaptic activation (Delling et al., 2002).

This study also characterizes FILIP mRNA and protein distribution during embryogenesis and in the adult mouse. It has been shown for the first time that FILIP mRNA and protein are expressed in the adult cortex.

Filamin A is the most potent actin-cross-linking protein. Furthermore, it interconnects the actin network with membrane receptors. This is a way to provide both mechanical stability to the cell membrane and to maintain cell-cell and cell-matrix connections. Filamins thus facilitate the activation of local processes such as actin polymerization in response to signaling cascades (Stossel et al, 2001). Filamin A seems to be required in signaling pathways that mediate organogenesis in multiple systems during neuronal migration and embryonic development.

FILIP negatively regulates the function of Filamin A. When FILIP is overexpressed in explants, neurons fail to migrate altogether. It was thus suggested to play a role in the regulation of cortical cell migration (Nagano et al., 2002).

One may speculate that FILIP expression in the adult brain could be necessary to prevent neurons from migrating after they have reached their final destination, doing so by inducing a Filamin A degradation process.

This study also provides a first insight into the co-expression of potassium channel Kir3.2 and the Filamin A interacting protein FILIP in different tissues and brain regions during embryogenesis and in the adult mouse.

A putative FILIP/ Kir3.2 interaction links the hyperpolarizing and thus inhibitory Kir3.2 channel activity to the activity of a protein that negatively regulates cell motility.

However, the scarce data published to date does not allow for more speculations concerning the putative physiological relevance of this interaction.

VII. SUMMARY

The subject of the present study was an examination of putative concurrence of Kir3.2, FILIP, and MUPP1 expression and distribution in the mouse model.

Previous studies proposed that the neuronal cell adhesion molecule NCAM regulates the surface delivery of Kir3.2 via a common binding partner, shared by Kir3.2 and NCAM. Two putative Kir3.2 binding partners were found in a Yeast Two-Hybrid screening system: FILIP and MUPP1.

Since co-expression in the same cell is the minimal requirement for Kir3.2/FILIP and Kir3.2/MUPP1 interaction, Western Blot analysis, *In Situ* hybridization, and Immunohistochemistry of these three molecules were performed and compared to define regions of putative co-expression.

This study is the first to demonstrate that the potassium channel Kir3.2 and the PDZ protein MUPP1 are co-expressed in the brain on both the mRNA and protein level during embryogenesis and in the adult mouse and can thus possibly interact with each other.

PDZ proteins are protein-protein interaction modules that are involved in the assembly of supramolecular complexes and also in the trafficking of these interaction partners. Since further studies were able to additionally show an interaction between MUPP1 and NCAM, we now propose that MUPP1 may present the missing link to understanding the way in which NCAM regulates cell surface localization of Kir3.2.

This study also characterizes FILIP mRNA and protein distribution during embryogenesis and in the adult mouse. It was the first to show that FILIP mRNA and protein are expressed in the adult cortex. Furthermore, this study provides a first insight into the co-expression of potassium channel Kir3.2 and the Filamin A interacting protein FILIP on both mRNA and protein level in different tissues and brain regions during embryogenesis and in the adult mouse.

FILIP is a negative regulator of Filamin A, inducing Filamin A degradation processes. Since Filamin A is the most potent actin cross-linker, it was suggested that FILIP play a role in the regulation of cell migration, especially in the cortex. Besides this, no other function such as membrane trafficking has been assigned to FILIP.

The putative physiological relevance of this interaction remains to be elucidated in further studies.

VII. ZUSAMMENFASSUNG

In der vorliegenden Arbeit wurden die Expression und Verteilung der Proteine Kir3.2, FILIP und MUPP1 untersucht.

Auf Grund von früheren Studien der Arbeitsgruppe wurde postuliert, dass das neuronale Zelladhäsionsmolekül NCAM den Transport von Kir3.2 zur Zelloberfläche mit Hilfe eines gemeinsamen Bindungspartners von NCAM und Kir3.2 reguliert. Der daraufhin durchgeführte Yeast Two Hybrid Screen ergab zwei potentielle Bindungspartner für Kir3.2: FILIP und MUPP1.

Für weiterführende Arbeiten ist es notwendig zu untersuchen, inwieweit sich die Expressionsmuster von Kir3.2 mit den beiden Bindungspartnern überlappen, da eine grundlegende Voraussetzung für die Interaktion zwischen Kir3.2/FILIP und Kir3.2/ MUPP1 die Co- Expression dieser Proteine in der gleichen Zelle ist. Daher haben wir *In situ* -Hybridisierungen, Western Blot- und Immunhistochemie- Experimente von diesen drei Molekülen angefertigt und miteinander verglichen, um die Frage einer möglichen Co-Expression klären zu können.

Im Rahmen dieser Studie konnte erstmalig gezeigt werden, dass der Kalium-Kanal Kir3.2 und das PDZ Protein MUPP1 während der Embryogenese und in der adulten Maus in verschiedenen Geweben sowohl auf mRNA- als auch auf Protein- Ebene co-exprimiert werden.

PDZ Proteine sind Protein-Protein Interaktionsmodule, die supramolekulare Protein-komplexe formen, jedoch auch an dem intrazellulären Transport der interagierenden Proteine beteiligt sind. Da weitere Versuche unserer Arbeitsgruppe in der Lage waren, eine Interaktion zwischen MUPP1 und NCAM zu zeigen, postulieren wir somit MUPP1 als das gesuchte Bindeglied zwischen NCAM und Kir3.2.

Die vorliegende Arbeit charakterisiert des Weiteren die Verteilung der FILIP mRNA und des Proteins während der Embryonalentwicklung und in der adulten Maus. So war es erstmals möglich zu zeigen, dass die FILIP mRNA und Protein im adulten Kortex exprimiert werden. Diese Arbeit ermöglicht weiterhin einen ersten Einblick in die Co-Expression von Kir3.2 und FILIP während Embryogenese und in verschiedenen Geweben im adulten Tier sowohl auf mRNA- als auch auf Proteinebene.

FILIP induziert den Abbau von Filamin A, einem zytoskelettassoziierten Protein, welches das für die Zellmotilität unabdingbare Aktin quervernetzt. FILIP wird daher eine Rolle bei der Regulation von Zellmigration z.B. im Kortex zugesprochen.
Andere Funktionen von FILIP, wie beispielsweise bei der Regulation des intrazellulären Transports von Proteinen, wurden bislang nicht beschrieben. Die potentielle physiologische Relevanz dieser Interaktion bleibt daher offen für weitere Studien.

VIII. REFERENCES

Ashcroft, F. M., Harrison, D. E., and Ashcroft, S. J. (1984). Glucose induces closure of single potassium channels in isolated rat pancreatic beta-cells. Nature 312, 446-448.

Ashcroft, F. M. and Rorsman, P. (1989). Electrophysiology of the pancreatic beta-cell. Prog. Biophys. Mol. Biol. 54, 87-143.

Ausrubel, F.M. (1996). Current Protocols in Molecular Biology. New York: Greene Publishing Associates, Inc.

Bécamel, C., Figge, A., Poliak, S., Dumuis, A., Peles, E., Bockaert, J., Luebbert, H., Ullmer, C. (2001). Interaction of serotonin 5-HT_{2C} receptors with PDZ 10 of multi PDZ protein MUPP1. J. Biol. Chem. 276, 12974-12982.

Beggs, H. E., Baragona, S. C., Hemperly, J. J., and Maness, P. F. (1997). NCAM140 interacts with the focal adhesion kinase p125(fak) and the SRC- related tyrosine kinase p59(fyn). J. Biol. Chem. 272, 8310-8319.

Beggs, H. E., Soriano, P., and Maness, P. F. (1994). NCAM-dependent neurite outgrowth is inhibited in neurons from Fyn-minus mice. J. Cell Biol. 127, 825-833.

Brackenbury, R., Thiery, J. P., Rutishauser, U., and Edelman, G. M. (1977). Adhesion among neural cells of the chick embryo. I. An immunological assay for molecules involved in cell-cell binding. J. Biol. Chem. 252, 6835-6840.

Bruemmendorf, T. and Rathjen, F. G. (1994). Cell adhesion molecules. The immunoglobulin superfamily. Protein Profile 1, 951-1058.

Chan, K. W., Langan, M. N., Sui, J. L., Kozak, J. A., Pabon, A., Ladias, J. A., and Logothetis, D. E. (1996a). A recombinant inwardly rectifying potassium channel coupled to GTP- binding proteins. J. Gen. Physiol 107, 381-397.

Chan, K. W., Sui, J. L., Vivaudou, M., and Logothetis, D. E. (1996b). Control of channel activity through a unique amino acid residue of a G protein-gated inwardly rectifying K^+ channel subunit. Proc. Natl. Acad. Sci. U. S. A 93, 14193-14198.

Chevesich, J., Kreuz, A.J., and Montell, C. (1997). Requirement for the PDZ domain protein, INAD, for localization of the TRP store-operated channel to a signaling complex. Neuron 18, 95-105.

Cohen, N. A., Brenman, J. E., Snyder, S. H., and Bredt, D. S. (1996). Binding of the inward rectifier K^+ channel Kir 2.3 to PSD-95 is regulated by protein kinase A phosphorylation. Neuron 17, 759-767.

Cole, G. J. and Glaser, L. (1986). A heparin-binding domain from N-CAM is involved in neural cell-substratum adhesion. J. Cell Biol. 102, 403-412.

Cole, G. J., Loewy, A., Cross, N. V., Akeson, R., and Glaser, L. (1986). Topographic localization of the heparin-binding domain of the neural cell adhesion molecule N-CAM. J. Cell Biol. 103, 1739-1744.

Condeelis, J., Salisbury, J., Fujiwara, K. (1981). A new protein that gels F actin in the cell cortex of *Dictyostelium discoideum* . Nature 292, 161-163.

Condeelis, J., Geosits, J., Vahey, M. (1982). Isolation of a new actin-binding protein from *Dictyostelium discoideum.* Cell Motility 2, 273-285.

Cremer, H., Chazal, G., Goridis, C., and Represa, A. (1997). NCAM is essential for axonal growth and fasciculation in the hippocampus. Mol. Cell Neurosci. 8, 323-335.

Cunningham, B. A., Hemperly, J. J., Murray, B. A., Prediger, E. A., Brackenbury, R., and Edelman, G. M. (1987). Neural cell adhesion molecule: structure, immunoglobulin-like-domains, cell surface modulation, and alternative RNA splicing. Science 236, 799-806.

Delling, M., Wischmeyer, E., Dityatev, A., Sytnyk, V., Veh, R.W., Karschin, A., Schachner, M. (2002). The neural cell adhesion molecule regulates cell-surface delivery of G-protein-activated inwardly rectifying potassium channels via lipid rafts. J. Neurosci. 22, 7154-7164.

DiMagno, L., Dascal, N., Davidson, N., Lester, H. A., and Schreibmayer, W. (1996). Serotonin and protein kinase C modulation of a rat brain inwardly rectifying K^+ channel expressed in xenopus oocytes. Pflugers Arch. 431, 335-340.

Doherty, P., Barton, C. H., Dickson, G., Seaton, P., Rowett, L. H., Moore, S. E., Gower, H. J., and Walsh, F. S. (1989). Neuronal process outgrowth of human sensory neurons on monolayers of cells transfected with cDNAs for five human N-CAM isoforms. J. Cell Biol. 109, 789-798.

Doherty, P., Fazeli, M. S., and Walsh, F. S. (1995). The neural cell adhesion molecule and synaptic plasticity. J. Neurobiol. 26, 437-446.

Doherty, P., Fruns, M., Seaton, P., Dickson, G., Barton, C. H., Sears, T. A., and Walsh, F. S. (1990). A threshold effect of the major isoforms of NCAM on neurite outgrowth. Nature 343, 464-466.

Doherty, P., Skaper, S. D., Moore, S. E., Leon, A., and Walsh, F. S. (1992). A developmentally regulated switch in neuronal responsiveness to NCAM and N-cadherin in the rat hippocampus. Development 115, 885-892.

Doherty, P. and Walsh, F. S. (1992). Cell adhesion molecules, second messengers, and axonal growth. Curr. Opin. Neurobiol. 2, 595-601.

Doyle, E., Nolan, P. M., Bell, R., and Regan, C. M. (1992). Hippocampal NCAM180 transiently increases sialylation during the acquisition and consolidation of a passive avoidance response in the adult rat. J. Neurosci. Res. 31, 513-523.

Edelman, G. M., Cunningham, B. A., Gall, W. E., Gottlieb, P. D., Rutishauser, U., and Waxdal, M. J. (1969). The covalent structure of an entire gammaG immunoglobulin molecule. Proc. Natl. Acad. Sci. U. S. A 63, 78-85.

Fakler, B., Brandle, U., Glowatzki, E., Weidemann, S., Zenner, H. P., and Ruppersberg, J. P. (1995). Strong voltage-dependent inward rectification of inward rectifier K^+ channels is caused by intracellular spermine. Cell 80, 149-154.

Fakler, B., Brandle, U., Glowatzki, E., Zenner, H. P., and Ruppersberg, J. P. (1994). Kir2.1 inward rectifier K^+ channels are regulated independently by protein kinases and ATP hydrolysis. Neuron 13, 1413-1420.

Fields, R. D. and Itoh, K. (1996). Neural cell adhesion molecules in activity-dependent development and synaptic plasticity. Trends Neurosci. 19, 473-480.

Fox, J.W., Lamperti, E.D., Eksioglu, Y.Z., Hong, S.E., Feng, Y., Graham, D.A., Scheffer I.E., Dobyns, W.B., Hirsch, B.A., Radtke, R.A., Berkovic, S.F., Huttenlocher, P.R., Walsh, C.A. (1998). Mutations in Filamin 1 prevent migration of cerebral cortical neurons in periventricular heterotopia. Neuron 21, 1315-1325.

Griffon, N., Jeanneteau, F., Prieur, F., Diaz, J., and Sokoloff, P. (2003). CLIC6, a member of the intracellular chloride channel family, interacts with dopamine D_2-like receptors. Mol. Brain Research 117, 47-57.

Hall, R.A., Premont, R.T., Chow, C.W., Blitzer, J.T., Pitcher, J.A., Claing, A., Stoffel, R.H., Barak, L.S., Shenolikar, S., Weinman, E.J., Grinstein, S., and Lefkowitz, R.J. (1998). The β_2-adrenergic receptor interacts with the Na^+/H^+-exchanger regulatory factor to control Na^+/H^+ exchange. Nature 392, 626-630.

Hamazaki, Y., Itoh, M., Sasaki, H., Furuse, M., and Tsukita, S. (2001). Multi-PDZ domain protein 1 (MUPP1) is concentrated at tight junctions through its possible interaction with Claudin-1 and junctional adhesion molecule. J. Biol. Chem. 277, 455-461.

Hartwig, J. and Stossel, T. (1975). Isolation and properties of actin, myosin, and a new actin-binding protein in rabbit alveolar macrophages. J. Biol. Chem. 250, 5696- 5705.

Henry, P., Pearson, W. L., and Nichols, C. G. (1996). Protein kinase C inhibition of cloned inward rectifier (HRK1/KIR2.3) K^+ channels expressed in Xenopus oocytes. J. Physiol. 495 (Pt 3), 681-688.

Hoffman, S. and Edelman, G. M. (1983). Kinetics of homophilic binding by embryonic and adult forms of the neural cell adhesion molecule. Proc. Natl. Acad. Sci. U. S. A 80, 5762-5766.

Hsueh, YP., Kim E, Sheng M. (1997). Disulfide-linked head-to-head multimerization in the mechanism of ion channel clustering by PSD-95. Neuron 18(5), 803-14.

Hynes, R. O. (1992). Integrins: versatility, modulation, and signaling in cell adhesion. Cell 69, 11-25.

Inanobe, A., Yoshimoto, Y., Horio, Y., Morishige, K. I., Hibino, H., Matsumoto, S., Tokunaga, Y., Maeda, T., Hata, Y., Takai, Y., and Kurachi, Y. (1999). Characterization of G-protein-gated K^+ channels composed of Kir3.2 subunits in dopaminergic neurons of the substantia nigra. J. Neurosci. 19, 1006-1017.

Inoue, H., Nojima, H., and Okayama, H. (1990). High efficiency transformation of Escherichia coli with plasmids. Gene 96, 23-28.

Isomoto, S., Kondo, C., and Kurachi, Y. (1997). Inwardly rectifying potassium channels: their molecular heterogeneity and function. Jpn. J. Physiol 47, 11-39.

Jeansonne, B., Lu, Q., Goodenough, D.A., and Chen, Y.H. (2003). Claudin-8 interacts with multi-PDZ domain protein 1 (MUPP1) and reduces paracellular conductance in epithelial cells. Cell. Mol. Biol. (Noisy-le-grand) 49, 13-21.

Jelacic, T. M., Kennedy, M. E., Wickman, K., and Clapham, D. E. (2000). Functional and biochemical evidence for G-protein-gated inwardly rectifying K^+ (GIRK) channels composed of GIRK2 and GIRK3. J. Biol. Chem. 275, 36211-36216.

Jiao, Y., Sun Z, Lee T, Fusco FR, Kimble TD, Meade CA, Cuthbertson S, Reiner A. (1999). A simple and sensitive antigen retrieval method for free-floating and slide-mounted tissue sections. J Neurosci Methods 93:149-162

Jorgensen, O. S. (1995). Neural cell adhesion molecule (NCAM) as a quantitative marker in synaptic remodeling. Neurochem. Res. 20, 533-547.

Jugloff, D.G., Khanna, R., Schlichter, L.C., Jones, O.T. (2000). Internalization of the Kv1.4 potassium channel is suppressed by interaction with PSD95. J. Biol. Chem. 275, 1357-1364.

Kadmon, G., Kowitz, A., Altevogt, P., and Schachner, M. (1990). Functional cooperation between the neural adhesion molecules L1 and N- CAM is carbohydrate dependent. J. Cell Biol. 110, 209-218.

Karschin, C. and Karschin, A. (1997). Ontogeny of Gene Expression of Kir Channel Subunits in the Rat. Mol. Cell Neurosci. 10, 131-148.

Kim, E. and Sheng, M. (2004). PDZ domain proteins of synapses. Nat. Rev. Neuroscience 2004 Oct.; 5(10): 771-81

Kimber, W.A., Trinkle-Mulcahy, L., Cheung, P.C.F., Deak, M., Marsden, L.J., Kieloch, A., Watt, S., Javier, R.T., Gray, A., Downes, C.P., Lucocq, J.M., and Alessi, D.R. (2002). Evidence that the tandem-pleckstrin–homology-domain-containing protein TAPP1 interacts with Ptd(3,4)P_2 and the multi-PDZ-domain-containing protein MUPP1 in vivo. Biochem. J. 361, 525-536.

Kofuji, P., Davidson, N., and Lester, H. A. (1995). Evidence that neuronal G-protein-gated inwardly rectifying K^+ channels are activated by G beta gamma subunits and function as heteromultimers. Proc. Natl. Acad. Sci. U. S. A 92, 6542-6546.

Kolkova, K., Novitskaya, V., Pedersen, N., Berezin, V., and Bock, E. (2000a). Neural cell adhesion molecule-stimulated neurite outgrowth depends on activation of protein kinase C and the Ras-mitogen-activated protein kinase pathway. J. Neurosci. 20, 2238-2246.

Kolkova, K., Pedersen, N., Berezin, V., and Bock, E. (2000b). Identification of an amino acid sequence motif in the cytoplasmic domain of the NCAM-140 kDa isoform essential for its neuritogenic activity. J. Neurochem. 75, 1274-1282.

Kozlov, G., Gehring, K., Ekiel, I. (2000). Solution structure of the PDZ2 domain from human phosphatase hPTP1E and its interactions with C-terminal peptides from the Fas receptor. Biochemistry 39(10), 2572-80.

Krapivinsky, G., Gordon, E. A., Wickman, K., Velimirovic, B., Krapivinsky, L., and Clapham, D. E. (1995). The G-protein-gated atrial K^+ channel IKACh is a heteromultimer of two inwardly rectifying K(+)-channel proteins. Nature 374, 135-141.

Krushel, L. A., Cunningham, B. A., Edelman, G. M., and Crossin, K. L. (1999). NF-kappaB activity is induced by neural cell adhesion molecule binding to neurons and astrocytes. J. Biol. Chem. 274, 2432-2439.

Kubo, Y., Baldwin, T. J., Jan, Y. N., and Jan, L. Y. (1993). Primary structure and functional expression of a mouse inward rectifier potassium channel. Nature 362, 127-133.

Kumar, R. and Shieh, B.-H. (2001). The second PDZ domain of INAD is a type I domain involved in binding to eye protein kinase C. J. Biol. Chem. 276, 24971-24977.

Laemmli, U. K. (1970). Cleavage of structural proteins during the assembly of the head of bacteriophage T4. Nature 227, 680-685.

Lee, S.S., Glaunsinger, B., Mantovani, F., Banks, L., and Javier, R. (2000). Multiple PDZ domain containing protein MUPP1 is a cellular target for both adenovirus E4-ORF1 and high-risk papillomavirus type 18 E6 oncoproteins. J. of Virology 74, 9680-9693.

Lesage, F., Guillemare, E., Fink, M., Duprat, F., Heurteaux, C., Fosset, M., Romey, G., Barhanin, J., and Lazdunski, M. (1995). Molecular properties of neuronal G-protein-activated inwardly rectifying K^+ channels. J. Biol. Chem. 270, 28660-28667.

Little, E. B., Crossin, K. L., Krushel, L. A., Edelman, G. M., and Cunningham, B. A. (2001). A short segment within the cytoplasmic domain of the neural cell adhesion molecule (N-CAM) is essential for N-CAM-induced NF-kappa B activity in astrocytes. Proc. Natl. Acad. Sci. U. S. A 98, 2238-2243.

Luescher, C., Jan, L. Y., Stoffel, M., Malenka, R. C., and Nicoll, R. A. (1997). G protein-coupled inwardly rectifying K^+ channels (GIRKs) mediate postsynaptic but not presynaptic transmitter actions in hippocampal neurons. Neuron 19, 687-695.

Mackie, K., Sorkin, B. C., Nairn, A. C., Greengard, P., Edelman, G. M., and Cunningham, B.A. (1989). Identification of two protein kinases that phosphorylate the neural cell-adhesion molecule, N-CAM. J. Neurosci. 9, 1883-1896.

Mancini, A., Koch, A., Stefan, M., Niemann, H., and Tamura, T. (2000). The direct association of the multiple PDZ domain containing protein MUPP1 with the human c-Kit C-terminus is regulated by tyrosine kinase activity. FEBS Letters 482, 54-58.

Mark, M. D. and Herlitze, S. (2000). G-protein mediated gating of inward-rectifier K^+ channels. Eur. J. Biochem. 267, 5830-5836.

Nagano, T., Yoneda, T., Hatanaka, Y., Kubota, C., Murakami, F., Sato, M. (2002). Filamin A-interacting protein (FILIP) regulates cortical cell migration out of the ventricular zone. Nat. Cell Biol. (4), 495-501.

Nehring, R.B., Wischmeyer, E., Doring, F., Veh, R.W., Sheng, M., Karschin, A. (2000). Neuronal inwardly rectifying potassium channels differentially couple to PDZ proteins of the PSD95/SAP90 family. J. Neurosci. 20 (1), 156-162.

Nourry, C., Grant, S.G.N., and Borg, J.P. (2003). PDZ domain proteins: plug and play! Sci STKE 179, RE7.

Orr, H. T., Lancet, D., Robb, R. J., Lopez de Castro, J. A., and Strominger, J. L. (1979). The heavy chain of human histocompatibility antigen HLA-B7 contains an immunoglobulin-like region. Nature 282, 266-270.

Parker, L.L., Backstrom, J.R, Sanders-Bush, E., and Shieh, B.-H. (2003). Agonist-induced phosphorylation of the Serotonin 5-HT_{2C} receptor regulates its interaction with multiple PDZ Protein 1. J. Biol. Chem. 278, 21576-21583.

Poliak, S., Matlis, S., Ullmer, C., Scherer, S. S., and Peles, E. (2002). Distinct claudins and associated PDZ proteins form different autotypic tight junctions in myelinating Schwann cells. J. Cell Biol. 159, Number 2, 361-371.

Probstmeier, R., Kuhn, K., and Schachner, M. (1989). Binding properties of the neural cell adhesion molecule to different components of the extracellular matrix. J. Neurochem. 53, 1794-1801.

Reichardt, L. F. and Tomaselli, K. J. (1991). Extracellular matrix molecules and their receptors: functions in neural development. Annu. Rev. Neurosci. 14, 531-570.

Robertson, S.P., Twigg, S.R., Sutherland-Smith, A.J., Biancalana, V., Gorlin, R.J., Horn, D., Kenwrick, S.J., Kim, C.A., Morava, E., Newbury-Ecob, R., Orstavik, K.H., Quarrell, O.W., Schwartz, C.E., Shears, D.J., Suri, M., Kendrick-Jones, J., Wilkie, A.O (2003). Localized mutations in the gene encoding the cytoskeletal protein filamin A cause diverse malformations in humans. Nat Genet. 33(4), 487-91.

Roche, K.W., Standley, S., McCallum, J., Dunely, C., Ehlers, M.D., Wenthold, R.J. (2001). Molecular determinants of NMDA receptor internalization. Nat. Neurosci. 4(8), 794-802.

Rutishauser, U. and Jessell, T. M. (1988). Cell adhesion molecules in vertebrate neural development. Physiol Rev. 68, 819-857.

Rutishauser, U. (1990). Neural cell adhesion molecule as a regulator of cell-cell interactions. Adv. Exp. Med. Biol. 265, 179-183.

Saffell, J. L., Williams, E. J., Mason, I. J., Walsh, F. S., and Doherty, P. (1997). Expression of a dominant negative FGF receptor inhibits axonal growth and FGF receptor phosphorylation stimulated by CAMs [published erratum appears in Neuron 1998 Mar;20(3):619]. Neuron 18, 231-242.

Saiki, R. K., Gelfand, D. H., Stoffel, S., Scharf, S. J., Higuchi, R., Horn, G. T., Mullis, K. B., and Erlich, H. A. (1988). Primer-directed enzymatic amplification of DNA with a thermostable DNA polymerase. Science 239, 487-491.

Sambrook, J., Fritsch, E. F., and Maniatis, T. (1989). Molecular cloning: A Laboratory Manual. (Cold Spring Habor: Cold Spring Habor Laboratory).

Sanes, J. R. (1989). Extracellular matrix molecules that influence neural development. Annu. Rev. Neurosci. 12, 491-516.

Schachner, M. (1991). Cell surface recognition and neuron-glia interactions. Ann. N.Y. Acad. Sci. 633, 105-112.

Schachner, M. (1997). Neural recognition molecules and synaptic plasticity. Curr. Opin. Cell Biol. 9, 627-634.

Shawn Xu, X.-Z., Choudhury, A., Li, X., and Montell, C. (1998). Coordination of an array of signaling proteins through homo- and heteromeric interactions between PDZ domains and target proteins. J. Cell Biol. 142, 545-555.

Sheng, M. and Sala, C. (2001). PDZ domains and the organization of supramolecular complexes. Annu. Rev. Neurosci. 24, 1-29.

Sitek, B., Poschmann, G., Schmidtke, K., Ulmer, C., Maskri, L., Andriske, M., Stichel, C.C., Zhu, X.-R., Luebbert, H. (2003). Expression of MUPP1 protein in mouse brain. Brain Research 970, 178-187.

Slesinger, P. A., Reuveny, E., Jan, Y. N., and Jan, L. Y. (1995). Identification of structural elements involved in G protein gating of the GIRK1 potassium channel. Neuron 15, 1145-1156.

Songyang Z, Fanning AS, Fu C, Xu J, Marfatia SM, Chishti AH, Crompton A, Chan AC, Anderson JM, Cantley LC. (1997). Recognition of unique carboxyl-terminal motifs by distinct PDZ domains. Science 275(5296), 73-7.

Springer, T. A. (1990). Adhesion receptors of the immune system. Nature 346, 425-434.

Stevens, E. B., Woodward, R., Ho, I. H., and Murrell-Lagnado, R. (1997). Identification of regions that regulate the expression and activity of G protein-gated inward rectifier K^+ channels in Xenopus oocytes. J. Physiol 503 (Pt 3), 547-562.

Stossel, T.P., Condeelis, J., Cooley, L., Hartwig, J.H., Noegel, A., Schleicher, M., Shapiro, S.S. (2001). Filamins as integrators of cell mechanics and signaling. Nature Reviews Mol. Cell Biol. 2, 138-145.

Takeichi, M. (1991). Cadherin cell adhesion receptors as a morphogenetic regulator. Science 251, 1451-1455.

Thiery, J. P., Brackenbury, R., Rutishauser, U., and Edelman, G. M. (1977). Adhesion among neural cells of the chick embryo. II. Purification and characterization of a cell adhesion molecule from neural retina. J. Biol. Chem. 252, 6841-6845.

Thomas, U., Kim, E., Kuhlendahl, S., Koh, Y. H., Gundelfinger, E. D., Sheng, M., Garner, C. C., and Budnik, V. (1997). Synaptic clustering of the cell adhesion molecule fasciclin II by discs- large and its role in the regulation of presynaptic structure. Neuron 19, 787-799.

Towbin, H., Staehelin, T., and Gordon, J. (1979). Electrophoretic transfer of proteins from polyacrylamide gels to nitrocellulose sheets: procedure and some applications. Proc. Natl. Acad. Sci. U. S. A 76, 4350-4354.

Ullmer, C., Schmuck, K., Figge, A., Luebbert, H. (1998). Cloning and characterization of MUPP1, a novel PDZ domain protein. + FEBS Letters 424, 63-68.

Van der Flier, A., Sonnenberg, A. (2001). Structural and functional aspects of filamins. BBA 1538, 99-117.

Vargas, M., Sansonetti, P., and Guillén, N. (1996). Identification and cellular localization of the actin-binding protein from ABP-120 from *Entamoeba histolytica.* Mol. Microbiol. 22, 849-857.

Wang, W., Hebert, S. C., and Giebisch, G. (1997). Renal K^+ channels: structure and function. Annu. Rev. Physiol 59, 413-436.

Wickman, K. and Clapham, D. E. (1995). Ion channel regulation by G proteins. Physiol. Rev. 75, 865-885.

Williams, A. F. and Barclay, A. N. (1988). The immunoglobulin superfamily-domains for cell surface recognition. Annu. Rev. Immunol. 6, 381-405.

Williams, E. J., Mittal, B., Walsh, F. S., and Doherty, P. (1995). FGF inhibits neurite outgrowth over monolayers of astrocytes and fibroblasts expressing transfected cell adhesion molecules. J. Cell Sci. 108 (Pt 11), 3523-3530.

Wischmeyer, E., Doring, F., and Karschin, A. (1998). Acute suppression of inwardly rectifying Kir2.1 channels by direct tyrosine kinase phosphorylation. J. Biol. Chem. 273, 34063-34068.

Wischmeyer, E., Doring, F., Spauschus, A., Thomzig, A., Veh, R., and Karschin, A. (1997). Subunit interactions in the assembly of neuronal Kir3.0 inwardly rectifying K^+ channels. Mol. Cell Neurosci. 9, 194-206.

Wischmeyer, E. and Karschin, A. (1996). Receptor stimulation causes slow inhibition of IRK1 inwardly rectifying K^+ channels by direct protein kinase A-mediated phosphorylation. Proc. Natl. Acad. Sci. U. S. A 93, 5819-5823.

Yamzaki, M., Furuike, S., Ito, T. (2002). Mechanical response of single filamin A molecules and its role in the actin cytoskeleton. J. Muscle Cell Res. Cell Motility 23, 525-534.

IX. APPENDIX

1. Abbreviations

∅	"without", diameter
g	G-force
aa	Amino acid
A	Adenine
Acc	Accession number
Amp	Ampicillin
ATP	Adenosine triphosphate
bp	Base pairs
BSA	Bovine serum albumine
C	Cytosine
cDNA	Complementary deoxyribonucleic acid
C .elegans	*Caenorhabditis elegans*
CTP	Cytosine triphosphate
dATP	2'-Desoxyadenosinetriphosphate
dCTP	2'-desoxycytidinetriphosphate
DEPC	Diethylpyrocarbonate
dGTP	2'-Desoxyguanosinetriphosphate
D .melanogaster	*Drosophila melanogaster*
DMSO	Dimethylsulfoxide
DNA	Deoxyribonucleic acid
DNase	Deoxyribonuclease
dNTP	2'-deoxyribonucleotide-5'-triphosphate
DTT	Dithiothreitol
E. coli	*Escherichia coli*
EDTA	Ethylendiamintetraacetic acid
f.c.	Final concentration
G	Guanosine
h	human, hour

HEPES	2-(4-(2-Hydroxyethyl)-piperzino)-ethansulfonic acid
IB	Immunoblotting
IH	Immunohistochemistry
kb	kilo base pairs
Kir	K^+ inwardly rectifying channel
LB	Luria Bertani
MOPS	(4-(N-morpholino)-propan)-sulfonic acid
mRNA	Messenger ribonucleic acid
Nt	Mucleotide
O_D	Optic density
ORF	Open reading frame
PAGE	Polyacrylamide gel electrophoresis
PBS	Phosphate-buffered saline
PCR	Polymerase chain reaction
RIPA	Buffer radioimmunoprecipitation buffer
rpm	rounds per minute
RNA	Ribonucleic acid
RNase	Ribonuclease
RT	room temperature
SDS	Sodium dodecyl sulfate
T	Thymine
TABS	N-tris(Hydroxymethyl)methyl-3-aminopropane-sufonic acid
Tab.	Table
TBS	Tris-buffered saline
TE	Tris-EDTA
TEMED	N,N,N',N'-tetraethylenamine
T_m	melting temperature
TM	Transmembrane segment
Tris	Tris(-hydroxymethyl)-aminomethane
U	Unit (enzymatic)
V	Volt
v/v	Volume per volume
Vol.	Volume

w/v	Weight per volume
ZMNH	Zentrum für Molekulare Neurobiologie Hamburg

Amino acids were abbreviated using the one letter code.

2. Oligonucleotides

Nr.	Primer	Sequence (5`- 3`)	pos.	T_m	acc. number
1.	Filip up	CTC ACC ATG AGG AAG TCT TGG	2587-2607	59.8	*
2.	Filip dn	ATG CAG GCC TGT CTG CAA AC	2994-3013	59.4	*
3.	Kir3.2 AS	TCA CCC ATT CCT CTC CGT CAG TTC TTC CGG GTT CTT CTC TTC CTC TTC TG	1725-1676	77.6	U51122
4.	Kir3.2 S	CAG AAG AGG AAG AGA AGA ACC CGG AAG AAC TGA CGG AGA GGA ATG GGT G	1725-1676	77.6	U51122
5.	MUPP up	CTC AGA GTT GGG GAT AGG ATT G	5674-5695	60.3	AF326543.1
6.	MUPP dn	CAT CTT CTG CTG CTG CTC C	6022-6040	58.8	AF326543.1

* Filip does not have an accession number, as the mouse sequence is not included in data base. M. Delling cloned the following sequence from mouse brain library in 2002:

atgagatctcgaaatcaaggtggagaaagttcatctaatgggcatgtctcctgccccaagccctccatcatcagcagtgacggtggtaagggaccctca
gaagatgcaaaaaagaacaaggcaaatcggaaggggggaggatgatgtcatggcttccggaaccgtcaaacgccacctcaagccatcaggagagagt
gagaaaaagactaagaagcctctggagttatccaaggaggacctcatccagctcctgagcatcatggaaggggagctgcaggctcgagaagatgtcatc
cacatgctgaagacggagaagaccaagcccgaggttctggaggcgcattatggatctgcagaaccagagaaagtgcttcgagtcctgcaccgcgatgc
catccttgctcaggagaagtccataggagaagatgtctatgagaaacccatctcagagctggacagactggaggaaaagcagaaggagacataccgcc
gcatgctggagcagctgctgttggctgagaagtgtcacaggcgcaccgtgtacgagctggaaaacgagaagcacaagcacaccgactacatgaacaaga
gcgacgacttcaccaacctgctggagcaggagcgagagaggttgaaaaagctccttgagcaagaaaaggcttaccaagcccgcaaagaaaaggaaaac
gccaagcggctcaacaaacttcgggatgagcttgtgaaactcaagtccttcgcactcatgctggtggatgagaggcagatgcacatcgagcagctgggcct
gcagagtcagaaagtccaggacctcactcagaaactgagagaggaggaagaaaaactcaaagccatcacttacaagtccaaggaagaccgccagaaact
gctcaagttggaagtggacttcgaacacaaggcctcgaggttttcccaggagcacgaagagatgaacgccaagttggctaaccaagagtctcacaacagg
cagcttagactcaaactggttggcttatcgcaaaggatcgaggaactggaagagaccaataaaagtcttcagaaggccgaggaagagcttcaggagctgag
agataaaattgccaaaggggaatgtggaaactccagtctcatggcggaagtggaaagtctgcgcaagcgcgtgcttgagatggagggcaaggatgaaga
gatcactaagaccgaggcccagtgccgggagctgaagaagaagctccaagaggaagaacaccacagcaaggaacttagactagaagtggagaagctgc
agaagaggatgtctgaactggagaagctggaggaggccttcagccgcagcaagtcggaatgcacccagctccatttgaacctggagaaggagaagaacc
taaccaaagacctgctgaacgagctggaggtggtcaagagtcgggttaaagaactcgagtgctcggagagcagactggagaaggttgagttaagcctcaa

agacgacctcacgaagctgaagtccttcactgtgatgctggtggacgagaggaaaaacatgatggagaaaataaagcaagaagagaggaaggtggatgg
gttgaataaaaacttcaaggtggagcaggggaaggtgatggatgtgacggagaagctaatcgaggaaagcaagaagcttttaaaactcaagtctgaaatgg
aggaaaaggtgtatagtctgaccaaggagagggatgagctgatgggtaaactgagaagcgaagaagaaaggtcctgtgaactgagctgcagcgttgactt
gctaaagaagcggcttgatggcatagaggaggtggagagggaaatcaaccgaggcaggctgtgcaaggggtctgagttcacctgcccggaagccaataa
aatcagggaactgacgcttgaaatcgagagactgaagaagcggctccagcagctggaggtggtggaggggacttgatgaagaccgaggacgaatacg
accagttggagcagaaattcagaaccgagcaggataaggcaaatttcctctcccagcagctcgaggaaattaagcaccaaatggccaagaacaaagcca
tagagaaaggggaggctgtgagccaggaagccgagctgcgacacaggttccggatggaggaggctaaaagtcgtgacttacaggctgaggtgcaggct
cttaaagagaagatccacgagctgatgaacaaggaagatcagctctctcagctccaggtcgactattcggtccttcagcaaaggtttatggaagaagaaacta
agaacaagaacatggggagggaggtcctcaacctgaccaaagagctggagctttccaagcgctacagccgagctctcaggccgagtggaaatggccgaa
ggatggtggacgtacccgtggcctccactggggtgcagaccgaggcggtgtgcggggatgctgcggaggaggagaccccggctgtgttcatccgcaaat
ccttccaggaagaaaatcacatcatgagtaatcttcgacaggtaggcctgaagaaacccatggaacggtcctcggtcctcgacaggtatcccccagccgcc
aatgaactcaccatgaggaagtcttggattccttggatgagaaaaagagaaaacggaccctcagctccccaggagaaagggcccaggccaaaccagggt
acagggcaccctggcgagctggtcctagcacccaagcagggccagcccttgcacatccgtgtgacacctgatcacgagaacagcactgccaccctggag
atcacaagccccacatctgaagagtttttctcgagtaccaccgtcattcctaccttaggcaaccagaaaccacggatcaccataattccatcacccaatgtc
atgtcgcaaaagcccaaaagtgcagatcctactctcggcccagaacgagccatgtcccctgtcacgattactacaatttccagagagaagagcccagaaggt
ggaaggggcgcgtttgcagacaggcctgcatccccatccagataatgacggtgtcaacgtctgcagcgccccctgaaatcgctgtctctcctgactctcag
gaagtgcctatgggaaggactatcctcaaagttaccccggaaaaacaaactgttccaaccccatgcggaagtacaatgccaatgcgaatatcatcaccacg
gaagacaataaaattcacattcacctgggttctcagtttaagcgatctcccgggcctgcagcagcggaaggcgtgagtccagttatcacggtccggcctgtca
acgtaacagccgagaaggaggtttctacgggcacagtccttcgctctcccaggaaccacctctcttcaagacctggtgctaacaaagtgaccagcactataa
ccataaccccggtcacaacgtcatccacacgaggaacccaatcagtgtcaggacaagatgggtcatctcagcggcctacacccacccgcatccccatgtca
aaaggtatgaaagcaggaaagccagtagtggcagccccaggagcaggaaatctgaccaaattccagcctcgagctgagactcagtctatgaaaatagagc
tgaagaaatctgcagccagcagcactgcctctcttggaggggggaagggctga (1-3645)

3.0 Curriculum Vitae

Persönliche Daten

Name:	Mirja Mossekel
Geburtstag:	23.02.1980
Geburtsort:	Hamburg, Deutschland

Schulausbildung

1986	Einschulung in Hamburg
1990	Albrecht-Thaer-Gymnasium, Hamburg
1998	Abitur, Note 1.2

Akademischer Werdegang

Okt. 1999	Beginn des Medizinstudiums in Hamburg
	Aufnahme in die Studienstiftung des deutschen Volkes
Aug. 2001	Physikum, Note “gut”
Okt. 2001	Beginn der Promotion am ZMNH
März 2003	1. Staatsexamen, Note “gut“
März 2005	2. Staatsexamen, Note “gut”
März 2006	3. Staatsexamen

Beruflicher Werdegang

1998-1999	Freiwilliges Soziales Jahr, Costa Rica
Feb. 2000	Krankenpflegepraktikum, London
Aug. 2002	Famulatur Allgemeinmedizin, Schottland
Aug. 2003	Famulatur Gynäkologie, Charité- Klinikum, Berlin
März 2004	Famulatur Pathologie, Charité- Klinikum, Berlin
Juli 2004	Famulatur Anästhesie, Mount Sinai Hospital, New York
April 2005	Praktisches Jahr, Chirurgie, Kreisspital Männedorf, Schweiz
Aug. 2005	Praktisches Jahr, Gynäkologie, Albertinen- Krankenhaus, Hamburg
Dez. 2005	Praktisches Jahr, Innere Medizin, Marien- Krankenhaus, Hamburg

4.0 Danksagung

Ganz herzlich möchte ich Frau Prof. Melitta Schachner für die Überlassung dieser Arbeit, ihre stete Präsenz und unbedingte Ansprechbarkeit bei Fragen und Problemen aller Art danken.

Dr. Markus Delling, dessen Forschungseifer ansteckend ist, danke ich für die sehr engagierte Betreuung, auch über Ozeane hinweg.

Dr. Susanne Fehr für ihre Hilfe bei den *In situ* Experimenten, die ohne ihre langjährige Erfahrung sicher nicht hätten realisiert werden können.

Dr. Andrej Irintchev für die Hilfe bei den Immunhistochemie- Experimenten. Auch hier war es sein reicher Erfahrungsschatz, der das Anfertigen der Immunhistochemien erst ermöglichte.

Dr. Yong Wee Wong, für die Einführung in wissenschaftliches Arbeiten und in die Labortechniken.

Dr. Daniela Schneeberger dafür, dass sie mich unter ihre Fittiche genommen hat und die Zeit gefunden hat, Ideen auszutauschen und Korrektur zu lesen.

Den CTAs Peggy Putthoff und Achim Dahlmann, die unermüdlich dafür sorgen, dass Materialien beschafft werden, radioaktiver Abfall richtig lagert, kompetente Zellen vorhanden sind und vieles mehr.

Den Studenten Daniel, Athena und Claas danke ich für den Kir3.2 Y2H Screen und unzählige weitere Arbeiten, die den Grundstock für diese Arbeit gelegt haben.

Meinen Laborkollegen Christina, Claudia, John, Markus, Ulrich und Tanja, die mir jeden trüben Tag erhellt und für eine heitere Arbeitsatmosphäre gesorgt haben.

Allen Mitarbeitern des ZMNH für die nette Zusammenarbeit, stete Diskussionsbereitschaft und ihre unendliche Geduld.

Meinen Freunden dafür, dass sie mir, je nach Bedarf, meine Füße zurück auf den Boden oder die Welt auf den Kopf stellen.

Meiner Familie, immer.

5.0 Eidesstattliche Versicherung

Hiermit versichere ich ausdrücklich, dass ich die vorliegende Arbeit selbständig und ohne fremde Hilfe verfasst, andere als die von mir angegebenen Quellen und Hilfsmittel nicht benutzt und die aus den benutzten Werken wörtlich oder inhaltlich entnommenen Stellen einzeln nach Ausgabe (Auflage und Jahr des Erscheinens), Band und Seite des benutzten Werkes kenntlich gemacht habe.
Ferner versichere ich, dass ich die Dissertation bisher nicht einem Fachvertreter einer anderen Hochschule zur Überprüfung vorgelegt oder mich anderweitig um Zulassung zur Promotion beworben habe.

Hamburg, den 30.11.2005